

# **MODELLING OF MICRO ELECTRO DISCHARGE MACHINING IN AEROSPACE MATERIAL**

A Thesis Submitted to

**National Institute of Technology, Rourkela  
(Deemed University)**

In Partial fulfillment of the requirement for the degree of

Master of Technology

in

Mechanical Engineering

By

**UMESH KUMAR VISHWAKARMA**



**Department of Mechanical Engineering  
National Institute of Technology  
Rourkela -769 008 (India)  
2011**

# **MODELLING OF MICRO ELECTRO DISCHARGE MACHINING IN AEROSPACE MATERIAL**

A Thesis Submitted to

**National Institute of Technology, Rourkela  
(Deemed University)**

In Partial fulfillment of the requirement for the degree of

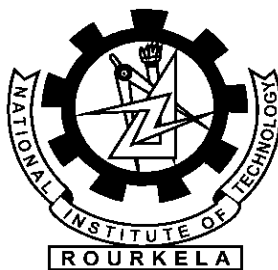
Master of Technology  
in  
Mechanical Engineering

By

**UMESH KUMAR VISHWAKARMA**

Under the guidance and supervision of

**Prof. K. P. MAITY**



**Department of Mechanical Engineering  
National Institute of Technology  
Rourkela -769 008 (India)  
2011**

*Dedicated to*

*My Most  
Loving Family*



**National Institute of Technology**

**Rourkela**

## **CERTIFICATE**

This is to certify that the thesis entitled “**MODELLING OF MICRO ELECTRO DISCHARGE MACHINING IN AEROSPACE MATERIAL**” submitted to the National Institute of Technology, Rourkela (Deemed University) by **Umesh Kumar Vishwakarma**, Roll No. **209ME2210** for the award of the Degree of **Master of Technology in Mechanical Engineering** with specialization in “**Production Engineering**” is a record of bonafide research work carried out by him under my supervision and guidance. The results presented in this thesis has not been, to the best of my knowledge, submitted to any other University or Institute for the award of any degree or diploma.

The thesis, in my opinion, has reached the standards fulfilling the requirement for the award of the degree of **Master of technology** in accordance with regulations of the Institute.

Place: Rourkela

**Dr. K. P. Maity**

Date:

Professor

Department of Mechanical Engineering  
National Institute of Technology, Rourkela

## ACKNOWLEDGEMENT

---

---

It is a great pleasure to express my gratitude and indebtedness to my supervisor Dr. **K. P. Maity**, Professor, Department of Mechanical Engg., for his guidance, encouragement, moral support and affection through the course of my work.

I am also grateful to Prof. **Sunil Kumar Sarangi**, Director, NIT, Rourkela who took keen interest in the work. My special thanks to Prof. **Ranjit Kumar Sahoo**, Head of Mechanical Engineering Department, Prof. **Siba Sankar Mahapatra**, Group Head and all staff members of the mechanical department for their timely help in completion of this work.

This work is also the outcome of the blessing, guidance, love and support of my family, this work could have been a distant dream if I did not get the moral encouragement from my elder brother Mr. **Ashok Vishwakarma** who believed me so much and provided me most convenient environment.

I feel pleased and privileged to fulfill my parent's ambition and I am greatly indebted to them for bearing the inconvenience during my M-Tech course. I express my appreciation to my friends for their understanding, patience and active co-operation throughout my M-Tech course finally.

**Date:**

**(Umesh Kumar Vishwakarma)**

## Nomenclature

EDM	Electrical discharge machining
MRR	Material removal rate (mm <sup>3</sup> /min)
P	Fraction of heat input to the workpiece
V	Voltage (V)
I	Current (A)
Q(r)	Heat flux (W/m <sup>2</sup> )
R	Spark radius (μm)
r	Radial coordinate
K	Thermal conductivity (W/mK)
T	Temperature variable (K)
T <sub>0</sub>	Initial temperature (K)
T <sub>on</sub>	Spark-on time (μs)
T <sub>off</sub>	Spark-off time (μs)
x,y	Cartesian coordinate of workpiece
C <sub>p</sub>	Specific heat (J/kgK)
C <sub>v</sub>	Crater volume (μm <sup>3</sup> )
NOP	Number of pulse

## **Abstract**

In this growing world of technology, design and manufacturing at the nano and micro level we need the things (product, service, design, technology) more accurate and defect free and on the same guidelines my thesis revolve around the same concept of advanced and precision manufacturing. Micro-manufacturing are extensively used for precision manufacturing with ease and error free. Present thesis work involve the use of multipurpose micro machine tool to do micro-EDM hole production on copper workpiece by using Micro-electric discharge machining, Micro-electric discharge machining is one of the advanced and precision manufacturing technology which deals with the micro manufacturing. It is used inproducts of aerospace, automobile and biomedical science industries. It can produce very accurate shapes with very small burrs much smaller than those produced by drilling and energy-beam processing. These parts do not need after-treatment processing such as deburring. It is essential for materials used in fuel nozzles, micro sensors, micro capsules, micro motors micro surgical instruments, micro robots, micro turbine and micro-moulds to resist wear, high temperature and high pressure micro manufacturing parts are widely used in the field of high performance micro machining technology. It can easily work on the hardest known substances with great ease and accuracy. It is also gaining popularity as a new alternative method to fabricate micro structures as it has low set up cost, high accuracy and large design freedom. It can fabricate three dimensional structures with great ease compared to etching or other methods with high aspect ratio. In the present investigation optimization of micro EDM has been carried by considering process parameters like voltage, current and pulse-on time and responses overcut, machining time, circularity error and burr size using  $L_4$  orthogonal array and design has been optimized by grey based taguchi method. FEA modelling of micro EDM process has also been carried out to predict the MRR and residual stress for single discharge. Multi-discharge MRR modelling has also been carried out for the micro EDM process and results are verified with the experimental investigation. Effects of different process parameters have also been studied.

# Table of Contents

CERTIFICATE .....	i
ACKNOWLEDGEMENT .....	ii
Nomenclature.....	iii
Abstract .....	iv
List of Figures .....	vii
List of Tables .....	ix
1. Introduction .....	1
2. Literature review .....	6
2.1 Literature based on different process parameters .....	6
Dielectric fluid: .....	6
Tool or electrode.....	7
Workpiece materials .....	8
Pulse generator.....	8
Polarity .....	9
Feed mechanism .....	9
2.2 Literature based on performance improvement .....	10
MRR improvement .....	10
Improving surface finish.....	11
Reduced tool wear.....	11
2.3 Literatures on hybrid micro EDM .....	12
3 Modelling of micro EDM.....	14
3.1 Thermal models of EDM and Micro-EDM.....	14
3.1.1 Assumptions .....	14
3.1.2 Governing equation.....	14
3.1.3 Heat distribution .....	14



3.1.4	Boundary conditions .....	15
3.1.5	Material properties .....	16
3.1.6	Heat flux .....	17
3.1.7	Modelling procedure using ANSYS .....	17
3.2	MRR modeling of micro EDM for single discharge .....	18
3.3	MRR calculation of micro EDM for multi-discharge .....	19
3.4	Residual Stress Analysis .....	20
4	Experimental Details .....	23
4.1	Specifications of AGIE250c .....	24
4.2	Taguchi method .....	25
4.3	Grey relational analysis .....	26
5.	Results and discussion .....	29
5.1.	Optimization of micro EDM .....	29
5.2	ANSYS model validation .....	34
5.3	MRR modelling of micro EDM for single discharge .....	36
5.4	Residual stress analysis .....	39
5.5	Optimization of model for micro EDM process .....	43
5.6	MRR modeling for multi-discharge experiment .....	46
5.6.1	Calculation of MRR .....	46
5.7	Effect of different process parameters .....	48
5.7.1	Effect of current .....	48
5.7.2	Effect of pulse duration .....	48
5.7.3	Effect of heat input to the workpiece .....	52
	Conclusions .....	59
	References .....	60

## List of Figures

Figure 1 Classification of micro-machining .....	1
Figure 2 Phase of electrical discharges [17] .....	5
Figure 3 An axisymmetric model for the EDM process simulation .....	15
Figure 4 Crater volume calculation.....	19
Figure 5 Flow chart for the procedure used to obtain the thermal and residual stresses .....	21
Figure 6 AGIE 250c .....	23
Figure 7 Test specimen .....	25
Figure 8 Drilled micro holes on Inconel 718 with different parameter settings.....	29
Figure 9 SEM image of micro hole at $V = 2V$ , $I = 3A$ and $T_{on} = 2\mu s$ .....	30
Figure 10 SEM image of micro hole at $V = 2V$ , $I = 5A$ and $T_{on} = 4\mu s$ .....	30
Figure 11 SEM image of micro hole at $V = 6V$ , $I = 3A$ and $T_{on} = 4\mu s$ .....	31
Figure 12 SEM image of micro hole at $V = 6V$ , $I = 5A$ and $T_{on} = 2\mu s$ .....	31
Figure 13 S/N ratio plot for overall grey relational grade.....	33
Figure 14 Main effect plots .....	33
Figure 15 Interaction plot .....	34
Figure 16 Nodal temperature distribution in 5 Cr die steel for EDM process .....	35
Figure 17 Temperature distribution in Inconel 718 with $V=20V$ , $I=1.5A$ and $P=0.08$ .....	36
Figure 18 Temperature distribution in Inconel 718 with $V=20V$ , $I=3A$ and $P=0.15$ .....	36
Figure 19 Temperature distribution in Inconel 718 with $V=20V$ , $I=5A$ and $P=0.20$ .....	37
Figure 20 Temperature distribution in Inconel 718 with $V=25V$ , $I=1.5A$ and $P=0.15$ .....	37
Figure 21 Temperature distribution in Inconel 718 with $V=25V$ , $I=3A$ and $P=0.20$ .....	37
Figure 22 Temperature distribution in Inconel 718 with $V=25V$ , $I=5A$ and $P=0.08$ .....	38
Figure 23 Temperature distribution in Inconel 718 with $V=30V$ , $I=1.5A$ and $P=0.20$ .....	38
Figure 24 Temperature distribution in Inconel 718 with $V=30V$ , $I=3A$ and $P=0.08$ .....	38
Figure 25 Temperature distribution in Inconel 718 with $V=30V$ , $I=5A$ and $P=0.15$ .....	39
Figure 26 Residual stress distribution in Inconel 718 with $V=20V$ , $I=1.5A$ and $P=0.08$ .....	40
Figure 27 . Residual stress distribution in Inconel 718 with $V=20V$ , $I=3A$ and $P=0.15$ .....	40
Figure 28 Residual stress distribution in Inconel 718 with $V=20V$ , $I=5A$ and $P=0.2$ .....	40
Figure 29 Residual stress distribution in Inconel 718 with $V=25V$ , $I=1.5A$ and $P=0.15$ .....	41
Figure 30 Residual stress distribution in Inconel 718 with $V=25V$ , $I=3A$ and $P=0.2$ .....	41

Figure 31 Residual stress distribution in Inconel 718 with V=25V, I=5A and P=0.08 .....	41
Figure 32 Residual stress distribution in Inconel 718 with V=30V, I=1.5A and P=0.2 .....	42
Figure 33 Residual stress distribution in Inconel 718 with V=30V, I=3A and P=0.08 .....	42
Figure 34 Residual stress distribution in Inconel 718 with V=30V, I=5A and P=0.15 .....	42
Figure 35 S/N ratio plot For Overall Grey Relational Grade .....	45
Figure 36 Bowl shaped crater cavity at V=2V, I=3A and Ton =2 $\mu$ s .....	46
Figure 37 Live element after application of heat flux.....	47
Figure 38 The effect of current on the temperature distribution along the radial direction from the centerline for micro EDM at P = 0.08, Ton = 2 $\mu$ s, V = 20 V.....	49
Figure 39 The effect of current on the temperature distribution along the depth of workpiece at the centerline for micro EDM at P = 0.08, Ton = 2 $\mu$ s, V = 20 V. ....	50
Figure 40 The effect of pulse duration on the temperature distribution along the radial direction from the centerline for micro EDM at P = 0.08, I = 1.5 A, V = 20 V. ....	51
Figure 41 The effect of pulse duration on the temperature distribution along the depth of workpiece at the centerline for micro EDM at P = 0.08, I = 1.5 A, V = 20 V. ....	52
Figure 42 The effect of heat input to the workpiece on the temperature distribution along the radial direction from the center line for micro EDM at I = 1.5 A, Ton = 2 $\mu$ s, V = 20V .....	53
Figure 43 The effect of heat input to the workpiece on the temperature distribution along the depth of workpiece at the centerline for micro EDM at I = 1.5 A, Ton = 2 $\mu$ s, V = 20 V.....	54

## List of Tables

Table 1 Chemical composition and thermal properties of 5 Cr die steel .....	16
Table 2 Chemical composition and thermal properties of Inconel 718 .....	16
Table 3 Chemical composition and thermal properties of Titanium 15.....	17
Table 4 Process parameters used for experiment.....	24
Table 5 Taguchi's L4 orthogonal array.....	24
Table 6 Process parameters used for modelling (Micro EDM).....	28
Table 7 Taguchi L9 Array of process parameters for Micro EDM .....	28
Table 8 Experimental data.....	31
Table 9 Grey relational generation.....	32
Table 10 Grey relational coefficient of each performance characteristics (with $\psi=0.5$ ) .....	32
Table 11 Response table (mean) for overall Grey relational grade .....	32
Table 12 EDM process parameters .....	35
Table 13 Experimental data obtain from model of micro EDM.....	43
Table 14 Grey relational generation and Grey relational coefficient of each performance characteristics (with $\psi=0.5$ ).....	44
Table 15 Response table (mean) for overall Grey relational grade .....	45

# Chapter 1

## INTRODUCTION

## 1. Introduction

In the present day scenario the micro products play a crucial role in the field of biomedical, nuclear, defence, transportation and space application. The demand of micro products is also increases in all industrial applications for the reduction in consumption of energy and protection of environment from pollution. There are numbers of methods available for producing micro products. The term micro machining defines the process that manufactures products in range of 1 to 999 $\mu\text{m}$  [1]. Whole process of micro machining is divided into two groups (I) Mask-based process (II) Tool-based process, which is shown in fig. 1 [2].

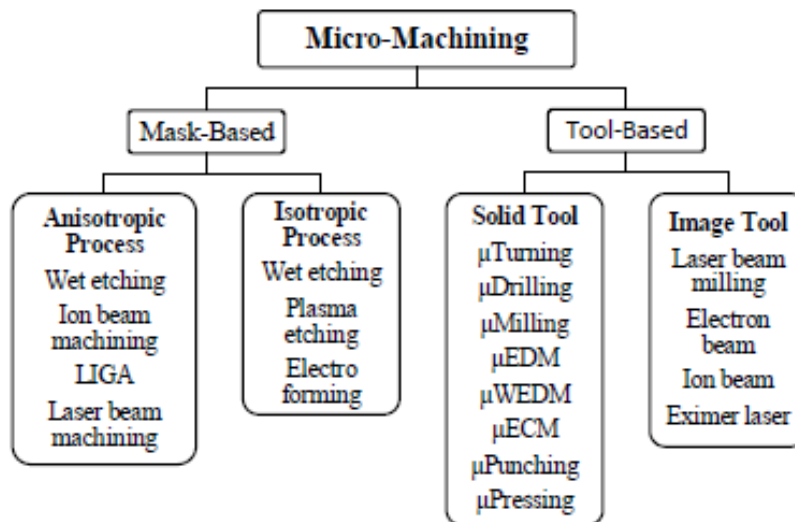


**Figure 1 Classification of micro-machining**

Micro Electrical discharge machining is a non-traditional concept of machining which has been widely used to produce dies and moulds. It is also used for finishing parts for aerospace and automotive industry and surgical components. In micro EDM, it is possible to machine feature smaller than 5  $\mu\text{m}$  and with Ra value less than 0.1 $\mu\text{m}$  [3]. Micro EDM is a thermal process, it utilizes spark to erode a conductive material. As there is no contact between tool and workpiece, there is no force acting between them. Therefore the process works efficiently, particularly in machining of difficult-to-cut materials. The micro-EDM operates on the same principle as that of EDM. Micro EDM has wide area of applications like in aerospace, nuclear, industrial, automobile, MEMS etc. In Electrical Discharge Machining the electrode is moved downward toward the work material until the spark gap (the nearest distance between both electrodes) small enough so that the impressed voltage is great enough to ionize the dielectric [4].

Micro Electro Discharge Machining is a market growing processing technology due to the industrial interest and the increasing number of applications. The process concept is not very different to conventional EDM. This fact makes easier to understand the features that can be machined. In spite of this, the process similarities, the process and the applied systems present some important differences with respect to conventional EDM.

Micro-electro-discharge machining (micro- EDM) is an attractive micro fabrication technique that can be used to cut any electrically conductive material, including steel, graphite, silicon [5], and magnetic materials [6], [7], including permanent magnets [8].

The most important difference between micro EDM and EDM (for both wire and die sinking EDM) is the dimension of the plasma channel radius that arises during the spark: in conventional EDM is much smaller than the electrode but the size is comparable for micro EDM [9].

Such small electrodes (WEDG can produce electrodes as small as  $\text{Ø}5\mu\text{m}$  and thin wires can be  $<\text{Ø}20\mu\text{m}$ ) present a limited heat conduction and low mass to dissipate the spark heat. An excessive spark energy can produce the wire rupture (or electrode burn in die sinking EDM), being the maximum applicable energy limited by this fact.

Together to the energy effects, the Flushing pressure acting on the electrode varies much with respect to the conventional process: the electrode pressure area is smaller but the electrode stiffness is lower, making it more “nervous”. The debris removal is more difficult because the gap is smaller, the dielectric viscosity is high and the pressure drop in micro volumes is higher.

As it happens in conventional EDM, the higher precision can be achieved only if electrode vibrations and wear are contained. This implies an important limitation for conventional EDM that turns out to be more restrictive in micro EDM.

For each discharge, the electrode wear in micro EDM is proportionally higher than conventional EDM. The electrode is softened, depending on the section reduction on the spark energy. For thin WEDM, the maximum traction force than can be applied to the wire will depend on the effective section and, therefore the traction control must be more accurate than that in conventional wires (0.20~0.33 mm) because the wire rupture can arise with fluctuations as small as 3~5 grams.

In micro EDM, the maximum Peak energy must be limited to control the unit removal rate per spark [10, 11] and use small electrodes and wires.

The balance between productivity, accuracy and spark energy reduction must be considered according to the application:

For high precision applications the energy must be reduced, For higher productivity, the energy per pulse must be increased, reducing the feeds (and the wire tension in WEDM).

Some key aspects to machine with small electrodes can be extracted from the presented ideas [10, 11]:

- Control the pulse energy
- Control the wire traction force (for WEDM)
- Increase the gap stability obtained by the control (avoid discharge fluctuations)
- Increase the machine positioning accuracy.

For micro EDM, the entire machine, the electrodes, the programme, the control, the measuring instruments and the operators play an important role in the process [12].

The basic principle of micro EDM is same as that of the EDM process. In EDM, a potential difference is applied between the tool and workpiece. Both the tool and the work material are to be electrically conductive, submerged in dielectric fluid. Generally kerosene or deionized water is used as the dielectric medium. The micro EDM system has a servo system with very high sensitivity and positional accuracy of  $\pm 0.5 \mu\text{m}$  [13]. Because of such precision it is possible to maintain a minimum gap of  $1 \mu\text{m}$  between tool and workpiece [14]. Depending upon the applied voltage and the gap between the tool and workpiece, an electric field would be established. The voltage applied to them must be enough to create an electric field higher than the dielectric rigidity of the fluid used in the process. There is no contact between the workpiece and the electrode so there is no mechanical vibration and chattering, electrically conductive material irrespective of any hardness can be machined.

As the electric field is established between the tool and the job, the plasma channel is formed between them. The electrical resistance of such plasma channel would be very less. Thus all of a sudden, a large number of electrons will flow from the tool to the job and ions from the job to the



tool. This is called avalanche motion of electrons. Such movement of electrons and ions can be visually seen as a spark. Thus the electrical energy is dissipated as the thermal energy of the spark.

The high speed electrons then impinge on the job and ions on the tool, and create a localized heat flux. Such intense localized heat flux leads to extreme instantaneous confined rise in temperature which would be in excess of 10,000°C. Such localized extreme rise in temperature leads to material removal. Material removal occurs due to instant vaporization of the material as well as due to melting. The molten metal is not removed completely but only partially.

As the potential difference is withdrawn the plasma channel is no longer sustained. As the plasma channel collapse, it generates pressure or shock waves, which evacuates the molten material forming a crater of removed material around the site of the spark. Due to the sudden decrease of internal pressure of the gas ball, the dielectric fluid breaks it making the ball to implode. As a consequence of this implosion, an ejection of molten metal is carried out and, afterwards, this ejected molten material solidifies in the form of little balls formed the so called EDM splinter or debris. In case of micro EDM the debris removal is complicated task, although some work have been done in this area also but still it is a prominent issue. Richardson et al. [15] has given a hydrodynamic flushing method utilizing self-generated bubbles for debris entrainment. Richardson et al. [16] has developed a wireless monitoring system to sense the debris accumulation.

Thus to summaries, the material removal in EDM mainly occurs due to formation of shock waves as the plasma channel collapse owing to discontinuation of applied potential difference. The different electric discharge phases have shown in Fig. 2 [17].

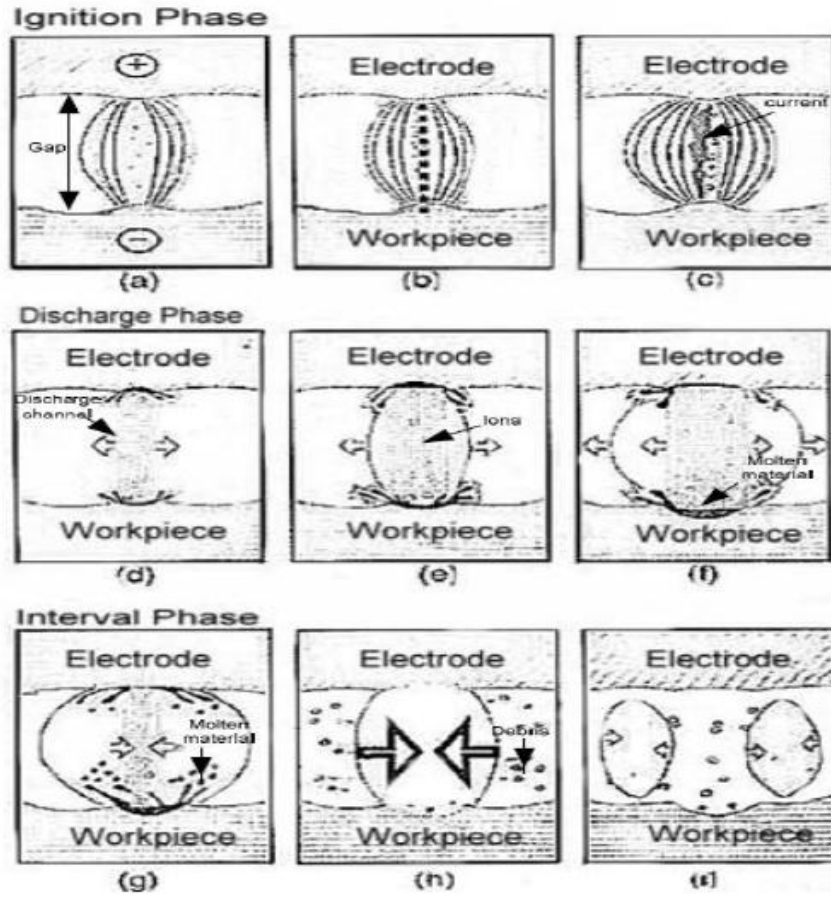


Figure 2 Phase of electrical discharges [17]

# Chapter 2

**LITERATURE REVIEW**

## 2. Literature review

There have been many researches done on the micro EDM. It has been decade's researchers working on the optimization of micro EDM process parameters and improving the performance. Micro EDM also assisted with different techniques to improve certain characteristics.

The whole review is divided into subgroups for better understanding about the investigations done by different investigators:

### 2.1 Literature based on different process parameters

**Dielectric fluid:** It is a nonconductive liquid that fills between the workpiece and electrode and remain nonconductive until needed space and voltage reaches. At that point dielectric fluid ionizes, becoming an electrical conductor and cause the current or spark to flow to the workpiece. The EDM setup consists of a power supply whose one lead is connected to the workpiece immersed in a tank having dielectric coil. The tank is connected to a pump, oil reservoir, and a filter system. The pump provides pressure for flushing the work area and moving the oil while the filter system removes and traps the debris in the oil. The oil reservoir restores the surplus oil and provides a container for draining the oil between the operations. The main functions of the dielectric fluid are:

- ✓ To flush the eroded particles produced during machining, from the discharge gap and remove the particles from the oil to pass through a filter system.
- ✓ To provide insulation in the gap between the electrode and the workpiece.
- ✓ To cool the section that was heated by the discharge machining.

The two most commonly used fluids are petroleum based hydrocarbon mineral oils and deionized water. The oils should have a high density and a high viscosity. These oils have the proper effects of concentrating the discharge channel and discharge energy but they might have a difficulty in flushing the discharge products.

There are so many works has been done using different dielectric fluids like Kerosene, de-ionized water. De ionized water generally has the advantage that faster metal removal rates can be realized. However the surface finish of the material is generally poorer than that which can be achieved when using oil [18]. Some powder also can be added to the dielectric to achieve a good compromise between higher MRR and lower surface finish. Sic powder of 3-5  $\mu\text{m}$  diameters

added to pure water which results in increased MRR [19]. Suspending micro-MoS<sub>2</sub> powder of grain size 2  $\mu\text{m}$  mixed kerosene, results in increased MRR and reduced surface roughness [20]. Dielectric mixed with graphite Nano-powder of 55 nm average particle sizes, has significantly improved the surface finish and high MRR with reduced TWR [21].

**Tool or electrode:** The tool material or electrode in a micro EDM process is mostly connected to the negative polarity so that less heat would be generated on the tool. The most used tool material is tungsten carbide [22, 23]. A LIGA fabricated array of 400 Cu electrodes with 20  $\mu\text{m}$  diameter was used to machine through-holes in 50  $\mu\text{m}$  thick stainless steel [24]. Micro electrodes are also fabricated by micro EDM grinding, in two steps rod electrodes of copper with diameter 3.0mm were cut to be 0.15mm on wire-EDM machine then EDM grinding process was used to grind micro-electrodes to fine diameter below 20 $\mu\text{m}$  on a CNC-EDM machine [25]. In the development of micro EDM a new phenomenon for making electrodes has been invented in which a 0.1mm tungsten electrode with 30–50A discharge current and several hundreds of micro seconds duration in single discharge was machined, a needle of 20–40 $\mu\text{m}$  in diameter has been formed instantaneously [26]. For machining the micro slit die, concave and rectangular shaped copper foils were combined piece by piece to form an assembled electrode. This die included 15 micro fins in a small tungsten carbide plate [27]. In batch mode production with the negative electrode, 3  $\times$  3 and 4  $\times$  4 tool electrode arrays are EDMed; 6  $\times$  6 and 16  $\times$  16 square holes array masks were fabricated in multi electrode arrays [28]. In investigation for obtaining high surface finish in the micro-EDM of WC using tungsten (W), copper tungsten (CuW) and silver tungsten (AgW) electrodes of 500  $\mu\text{m}$  diameter it has been found that AgW provides better electrical and thermal properties, smooth and shiny surfaces compared to other EDM electrodes [29]. Fabrication of high aspect ratio silicon micro electrode arrays has been done by micro-wire electrical discharge machining. Arrays with 144 electrodes on a 400  $\mu\text{m}$  pitch were machined on 6 and 10 mm thick p-type silicon wafers to a length of 5 and 9 mm, respectively [30]. UV-LIGA with the Micro electro-discharge machining process can fabricate high-aspect-ratio electrode array, and an easy and rapid process for fabricating ultra-thick SU-8 microstructures up to millimetre depth. First, the modified UV-LIGA process was used to fabricate the copper holes array, and then the hole array electrode was employed as a tool in the micro-EDM process to fabricate the multiple-tipped electrodes. The aspect ratio is up to 17.65 [31]. A novel machining technique has been used for micro-EDM that actuates the EDM electrode on an orbital trajectory

that is created by a 2-axis flexural micro-EDM head with a range of  $\pm 100 \mu\text{m}$  in both X and Y directions [32]. A new type of EDM tool micro electrode fabrication was developed using a combination of near UV lithography to directly polymerize a micro mould made of SU-8<sup>TM</sup> in combination with electroplating [33]. Tungsten micro-tools with a diameter ranging from  $1 \mu\text{m}$  to  $26 \mu\text{m}$  and aspect ratio ranging from 15 to 20 were obtained in about 30 minutes with a low cost and automated technique. This one is based on the electrochemical etching of the tool material with a process which has fully been integrated in a milling micro EDM machine [34].

**Workpiece materials:** The only necessary condition for workpiece in micro EDM is that it should be electrically conductive. There are many workpiece materials available on which different research work have been done like tungsten carbide, hardened steel X210Cr12 [35], tool steel P20, brass (Cu Zn 15) and aluminium (Al 5083) [36], stainless steel [37], molybdenum [38] etc. Hang et al. [39] studied the machinability of platinum metal by taking latent heat of fusion and evaporation into account firstly considering a general electrode wear compensation strategy. Pradhan et al. [40] investigated micro EDM for machining of titanium super alloys and the process parameters were optimized by Taguchi analysis. In machining of TC4 alloy different parameters have been studied and it is found that positive polarity machining is far superior to negative polarity machining. It is more optimal when open-circuit voltage, pulse width and pulse interval are 130 V,  $5 \mu\text{s}$  and  $15 \mu\text{s}$  respectively on the self-developed multi-axis micro-EDM machine tool. When flushing method is applied in micro-EDM, the machining efficiency is higher and relative wear of electrode is smaller [41]. Cemented carbide (WC-Co) and austenitic stainless steel (SUS 304) are two important materials used extensively in manufacturing because of their superior wear and corrosion resistance. The effect of discharge energy and electro-thermal material properties on the performance during the micro-EDM drilling of the above material has also been investigated [4].

**Pulse generator:** In conventional EDM where a static iso-energetic pulse generator uses a transistor to switch on/off DC power, provides short pulse-on time because of the long delay time for the discharge current to diminish to zero after detecting the occurrence of a discharge [42]. To avoid this resistance capacitance (RC) generators are used with a small capacitance of less than 1nF. RC generator is mainly applied in conventional micro EDM, although transistor type iso-pulse generator is more effective for obtaining higher MRR, with the new transistor type iso-pulse generator developed, the pulse duration can be reduced to about 30 ns [43]. Masuzawa

and Fujino [44] were the first to study the application of the transistor-type generator in micro-EDM, and they have obtained a pulse-on time of 220ns. Transistor-type pulse train generator is unsuitable for micro EDM due to its low removal rate: 80-ns and 30-ns pulse on-times of discharge current can be obtained by using the transistor-type isopulse generator and the removal rate of this generator is two or three times higher than that of the traditional RC pulse generator [45]. In the study of pulse condition affecting MRR and surface roughness it has been found that the voltage and current of the pulse exert strongly to the machining properties and the shorter EDM pulse is more efficient to make a precision part with a higher material removal rate, in the measurement of the gap between a tool and machined surface, it is increased with an increase of voltage and current. But it is inversely proportional to the length of pulse-on time [46]. Transistor serves as a switching device but it has some limitations because of this reason an alternative needed, MOSFET (Metal Oxide Semiconductor Field Effect Transistor) was found to be a suitable alternative [47]. MOSFETs have the advantage of high input impedance and absence of thermal runaway and second breakdown as compared to bipolar junction transistors [48]. A transistor-controlled power supply composed of a low energy discharge circuit and an iso-frequency pulse control circuit can provide the functions of high frequency and lower energy pulse control, by this the peak current decreases with an increase in pulse-control frequency with a 33.33% duty cycle [49].

**Polarity:** Normally, to obtain higher material removal rates in micro-EDM, the workpiece is usually set as the anode and the wire electrode as the cathode (straight polarity machining). This is because the discharge energy distributed to the anode is normally greater than that to the cathode [50]. The size of the discharge crater under the final finishing conditions with the reversed polarity is found about 0.8  $\mu\text{m}$  for tungsten and 1  $\mu\text{m}$  for super fine particles [51].

**Feed mechanism:** Feed mechanism is very essential factor to be considered to give micro feed to the electrodes; impact drive mechanism [52] and direct drive method [53] were proposed based on piezoelectric actuation. Piezoelectric/electrostrictive actuators are widely used in micro feeding and ultra-precision positioning, because of their fine resolution, rapid response, high generative force, and easy to miniaturization characteristics. Li et al. [54] proposed inchworm electrode feed mechanism having features like, high feeding accuracy and quick response to keep micro gap between electrode and workpiece during machining process. By integrating the transistor type isopulse generator with the servo feed control system, removal rate can be

increased by about 24 times than that of the conventional RC pulse generator with a constant feed rate in both semi finishing and finishing conditions [44]. The high-frequency response and the long working range are realized by the macro/micro-dual-feed spindle, which helps to keep the favourable discharge gap and ensure a long working range at the same time [55]. Muralidhara et al. [56] proposed a directly coupled piezo actuated tool feed mechanism; the proposed approach will be useful for real-time tool feed control providing compensation for tool wear to reach the desired depth of micromachining.

## 2.2 Literature based on performance improvement

Since micro EDM is a new machining process, a great deal of research work is being carried out to improve the accuracy of the process. The wear of electrode plays a critical role in improving the accuracy. The models for MEDM are still in developing stages. The research on micro EDM is focused also on the machining processes for electrode production. To find the optimal machining parameters is also of a great importance in the batch production. The optimal value of the current depends on the electrode size: greater the electrode higher the working and ignition current.

**MRR improvement:** Material removal phenomenon can be explained in two ways: one is vaporization and other is bubble explosion of superheated metal [57]. In bubble explosion process there will be increase in MRR due to increase in density. In the ultrasonic vibration assisted micro EDM, it has been found that vibration at 60% of the peak power with capacitance of 3300 pF gives the best MRR [58] as per the ANOVA analysis. Guha et al. [59] evaluated MRRs for copper & beryllium alloys with graphite and copper & tungsten electrodes (negative polarity) and copper electrode (positive and negative polarity). MRR was higher when positive polarity was used for copper electrodes. For negative polarity the highest MRR were obtained with graphite electrodes. Yan et al. [60] observed in their investigation that using negative polarity in EDM caused a higher MRR under a higher discharge energy ( $I_p > 3$  A or  $t_{on} > 5$  ms); in contrast, a positive polarity caused a higher MRR under lower discharge energy ( $I_p < 3$  A or  $t_{on} < 5$  ms). Kung et al. [61] studied the MRR and EWR during the conventional powder-mixed EDM (PMEDM) of cobalt bonded tungsten carbide (WC-Co) using Al powder of 1.5–2  $\mu$ m and 10–20 g/L. There are inherent problems associated with EDM machining process such as thermal



damage due to a large heat-affected zone (HAZ), high tool wear rate, low material removal rate, high surface roughness and poor dimensional accuracy, etc. [62-65].

**Improving surface finish:** Fong and Chen [66] investigated the effect of additives on surface quality of EDMed SKD-11. It has been found that greater the particle size will cause less surface finish. Al powder produces the best surface finishing of the machined work. Liu et al. [67] combined Micro EDM with high-frequency dither grinding (HFDG) to improve the surface roughness of micro-holes.

**Reduced tool wear:** The volumetric wear is defined as the ratio between the eroded volumes from the workpiece  $V_p$  and the volume lost due to the wear occurring on the electrode  $V_e$ . Due to wear in the electrodes achieving same dimension in repeatedly work is not possible even when using uniform wear method (UWM) of tool wear compensation [68] or the real-time wear compensation technique [69, 70]. Machining time can be significantly reduced by 40% when using the electrode wear compensation method, compared to the uniform wear method [71]. Yu et al. [68, 72–73] proposed the uniform wear method based on layer-by-layer machining to compensate for the longitudinal tool wear while maintaining the original electrode shape in micro-EDM with respect to cylindrical electrodes or electrodes with various sections. Rajurkar and Yu [74] presented a method of integrating an existing computer-aided design (CAD)/computer aided manufacturing system with the uniform wear method to machine complex three-dimensional (3D) micro shapes using simple shaped electrodes. Yu et al. [75] presented a theoretical model which accounts for the effect of tool wear for surface profile generation during each pass since the uniform wear method involves a time-consuming and empirical approach for selecting tool paths and machining parameters. Kozak et al. [76] presented two models of electrode shape deformation which take into consideration the effect of tool electrode wear. This study showed a good agreement of theoretical and experimental results of modelling of the rotary electrical discharge machining process. Pham et al. [36] proposed a simple method for volumetric wear ratio estimation in micro-EDM drilling based on geometrical information obtained from the machining process. Yeo and Tan [77] proposed drilling method that can compensate the tool wear and produce more accurate micro holes as compared to other methods. Uhlmann and Roehner [78] have worked on the reduction of wear of tool electrodes by using boron doped CVD-diamond (B-CVD) and polycrystalline diamond (PCD). Wang et al. [79] proposed a new type of electrode which is made by way of the electro-deposition process on

the basis of the difference between the discharging performance of the electrodeposited coating and that of the matrix to ensure uniform wear of electrode bottom faces. The results prove that Cu-ZrB<sub>2</sub> composite coating electrodes have better corrosion resistance than pure copper electrodes. For reducing wear some coatings are also being applied on the electrode, Nano crystalline coatings exhibited smaller discharge craters compared to those for microcrystalline diamond coatings, and microcrystalline coating showed melted material around the discharge crater [80]. PCD and B-CVD diamond as tool electrode materials for micro-die sinking EDM showed good results with respect to wear and process behaviour under process conditions of micro-EDM [79].

High aspect ratio: High aspect ratio micro fabrication is desired for producing practical micro components. By combining LIGA and Micro EDM the high aspect ratio microstructure can be produced [81]. Li et al. [55] with inch worm type of micro feed mechanism was able to obtain Micro electrode rod as small as 25  $\mu\text{m}$  and micro holes with minimum size of less than 50  $\mu\text{m}$ . The maximum aspect ratios of micro electrode rods and micro holes exceed 20 and 10 respectively. To machine micro holes with higher aspect ratio, the technique shaping an electrode rod with circular cross-section into one with non-circular cross-section is a feasible method [82]. WEDM can produce micro parts in a variety of conductive materials with aspect ratios up to 100 [83]. Cao et al. [84] demonstrated the replication of high-aspect-ratio micro scale structures in Al and Cu by compression molding with such surface-engineered Ta mould inserts.

### **2.3 Literatures on hybrid micro EDM**

Micro EDM assisted with different techniques can improve the performance significantly. Introduction of ultrasonic vibration causes phenomena such as acoustic streaming and results in better debris removal [85]. Masuzawa et al. introduced tool withdrawal and 2D vibration (sinusoidal motion of tool) to an EDM process for machining deep holes to increase the flushing effect [86, 87]. Introduction of ultrasonic vibration in micro EDM has been reported to improve the process performance [85, 88-90]. Gao and liu [91] also introduces ultrasonic vibration but in this it was given to the workpiece. Takahata et al. [92] combined micro EDM and LIGA technique, to fabricate high-aspect-ratio WC-Co micro structure having high resistance to buckling and wear when used as mechanical components or tools. Kuo et al. [93] integrated Micro-EDM (micro electro-discharge machining) with Nd-YAG laser as a novel process for

precise micro assembly. Yan et al. [23] combined micro EDM (MEDM) and micro ultrasonic vibration machining (MUSM). Yan et al. [90] developed three key techniques, (i) development of an open architecture CNC system with sub micro-meter resolution of a two-axis linear motor stage, (ii) development of a wire transport system and (iii) development of a power supply system, for a prototype CNC micro-wire EDM machine. Beltrami et al. [94] have developed a very precise EDM machine called Delta3 at EPFL and connected to a new generation EDM-generator from AGIE. It has a working volume of  $8\text{mm} \times 8\text{mm} \times 8\text{mm}$ , a high resolution (5 nm) and a high bandwidth dynamic (600 Hz). Guo et al. [95] developed two key components techniques for a CNC micro-EDM machine. Firstly, to achieve the motion control requirement of high precision, high sensitivity and hard real-time an open architecture CNC system is developed with sub micro-meter resolution of a 3axis linear motor stage. Secondly to deal with the difficulties in micro electrodes on-line fabrication and compensation, a machine vision system is developed with a resolution of  $1.61\ \mu\text{m}$  and a magnification is 113~729. Chern et al. [96] described the development of a novel micro-punching machine that is capable of producing precision micro-holes. By applying the vibration machining technique, efficiency of micro-EDM is enhanced, which is evident in the reduction of machining time and in the improved roundness of the die opening and the drilled micro-holes. Sundaram et al. [58] investigated the optimization of machining parameters on the MRR and tool wear in ultrasonic assisted micro EDM, with the help of Taguchi method. Yang et al. [97] combined micro EDM with LIGA to manufacture high aspect ratio electrode arrays. Yu et al. [98] presented a new method of drilling high aspect ratio micro-holes by EDM, in which the planetary movement of an electrode, with enhancement from ultrasonic vibration, provides an unevenly distributed gap for the debris and bubbles to escape from the discharge zone easily. Zilong et al. [99] investigated a new micromachining method for the fabrication of micro-metal structures by using micro-reversible electrical discharge machining. Lin et al. [100] proposed a technique to fabricate micro ball joint and bearings by micro-EDM and electroforming.

# Chapter 3

## MODELLING OF MICRO EDM

### 3 Modelling of micro EDM

In this study firstly one ANSYS model have been developed taking Shankar et al [101] as reference for EDM process, after matching results it is converted into a micro EDM model and in addition to 5 Cr die steel [101] thermal models for Inconel 718 and Titanium 15 also have been developed. Results from thermal analysis have been used for calculating and comparing MRR and also to study the effect of different process parameters on temperature isotherms.

#### 3.1 Thermal models of EDM and Micro-EDM

The principle of working for EDM and Micro EDM are same, the material is removed due to melting and vaporization caused by repetitive sparks between tool and workpiece. The following assumptions can be made:

##### 3.1.1 Assumptions

- The domain was axisymmetric.
- The material properties of the workpiece were temperature independent.
- The analysis is done for single spark.
- The ambient temperature was room temperature.
- The workpiece material was isotropic and homogenous.

##### 3.1.2 Governing equation

The governing equation of the heat conduction in axisymmetric model is given by

$$\rho C_p \left[ \frac{\partial T}{\partial t} \right] = \left[ \frac{1}{r} \frac{\partial}{\partial r} \left( K_r \frac{\partial T}{\partial r} \right) + \frac{\partial}{\partial z} \left( K \frac{\partial T}{\partial z} \right) \right]$$

Where  $\rho$  is density,  $C_p$  is specific heat,  $K$  thermal conductivity of the workpiece,  $T$  is the temperature,  $t$  is the time and  $r$  &  $z$  are coordinates of the workpiece.

##### 3.1.3 Heat distribution

Many authors have assumed a uniform disc source [102-105] for EDM. However Di Bitonto et al. [106-108] and Bhattacharya [109] have shown Gaussian heat distribution is more realistic

and accurate than disc heat source. In present study Gaussian heat distribution is considered. The Fig.3 shows a schematic diagram of thermal model with the applied boundary conditions.

### 3.1.4 Boundary conditions

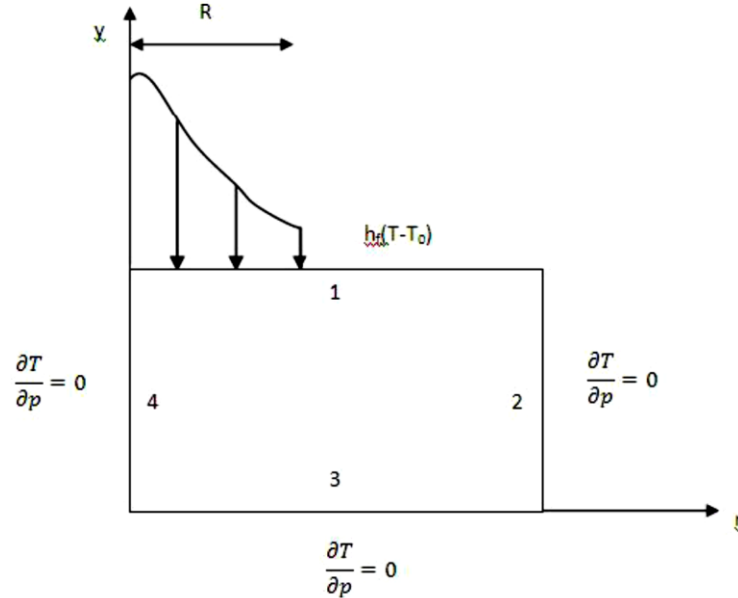


**Figure 3** An axisymmetric model for the EDM process simulation

On the top surface the heat is transferred to the workpiece shown by Gaussian hat flux distribution. Heat flux is applied on boundary 1 up to spark radius  $R$ , beyond  $R$  convection takes place due to dielectric fluids. As 2 & 3 are far from the spark location and also very short spark on time no heat transfer conditions have been assumed for them. For boundary 4, as it is axis of symmetry the heat flux is taken as zero.

In mathematical terms, the applied boundary conditions are given as follows:

$$K \frac{\partial T}{\partial z} = Q(r), \text{ When } R < r \text{ for boundary 1}$$

$$K \frac{\partial T}{\partial z} = h_f(T-T_0), \text{ When } R \geq r \text{ for boundary 1}$$

$$\frac{\partial T}{\partial p} = 0 \text{ For boundary 2, 3 \& 4.}$$

where  $h_f$  is heat transfer coefficient of dielectric fluid,  $Q(r)$  is heat flux due to the spark,  $T_0$  is the initial temperature and  $T$  is the temperature.

### 3.1.5 Material properties

The thermal properties and chemical composition of 5 Cr die steel, Inconel 718 and Titanium 15 are given in table 1, 2 and 3 respectively.

**Table 1 Chemical composition and thermal properties of 5 Cr die steel**

<b>Chemical composition</b>									
Element	Cr	Ni	C	Mn	Si	P	S	N	Mo
Content (%)	4-6	-	0.1 min	1	1	0.04	0.03	-	0.40–0.65
<b>Thermal properties</b>									
Thermal conductivity, K (W/mK)	48.5								
Specific heat, C (J/kgK)	425.0								
Density, $\rho$ (kg/m <sup>3</sup> )	8593								
Melting temperature (K)	2100								

**Table 2 Chemical composition and thermal properties of Inconel 718**

<b>Chemical composition</b>							
Element	Ni+Co	Cr	Fe	Nb+Ta	Mo	Ti	Al
Content (%)	50-55	17-21	BAL	4.75-5.5	2.8-3.3	.65-1.15	0.2-0.8
<b>Thermal properties</b>							
Thermal conductivity, K (W/mK)	14.5						
Specific Heat, C (J/kgK)	435						
Density, $\rho$ (kg/m <sup>3</sup> )	8190						
Melting temperature (K)	1609						

**Table 3 Chemical composition and thermal properties of Titanium 15**

<b>Chemical composition</b>							
Element	C	Fe	H	N	O	Ti	C
Content (%)	0.1	0.3	0.015	0.03	0.25	BAL	0.1
<b>Thermal properties</b>							
Thermal conductivity, K (W/mK)						7.62	
Specific Heat, C (J/kgK)						490	
Density, ρ (kg/m <sup>3</sup> )						4900	
Melting temperature (K)						1923	

### 3.1.6 Heat flux

A Gaussian heat flux distribution is assumed in present analysis.

$$Q(r) = \frac{4.45 PVI}{\pi R^2} \exp\left\{-4.5 \left(\frac{r}{R}\right)^2\right\}$$

where P is energy portion to the workpiece, V is the discharge voltage, I is current and R is spark radius.

Value of P mainly depends upon the material properties of the electrode. Value of P determined by yadav et al. [110] to be 0.08 for their work of conventional EDM. Shankar et al. [101] have calculated value of P about 0.4-0.5, using water as dielectric. The relevant values of process parameters used in this study are given in table. Spark on time, for the micro EDM process, of 2µs is divided into 10 sub steps, with initial condition set to room temperature. Temperature distribution during single spark has been calculated using ANSYS 12.0, and element those having temperature above the melting temperature were “killed” for calculation of MRR.

### 3.1.7 Modelling procedure using ANSYS

EDM is a complicated process that requires a powerful tool to simulate the process. In present analysis the simulation has been done on ANSYS 12.0 multi-physics. Analysis of any complex



geometry can be easily done using ANSYS. It has many finite element analysis capabilities, ranging from a simple, linear, static analysis to a complex, nonlinear, transient dynamic analysis in the fields such as structural mechanics, thermal systems, fluid mechanics, and electromagnetic.

For EDM analysis the geometry size taken as  $500 \mu\text{m} \times 500 \mu\text{m}$ , with a element size of  $10 \mu\text{m}$ . The process parameters used for EDM simulation are given in table 4. The following procedures have been followed. After EDM modelling the work is expanded for the micro EDM with different parameter setting as given in table 4.

Step 1: Start ANSYS 12.0.

Step 2: Units: S.I.

Step 3: Analysis method: Thermal, h method

Step 4: Problem domain: In this step, the geometry of the problem is created using ANSYS.

Two-dimensional workpiece geometry is created. However, the domain is axisymmetric about yaxis, dimensions of the workpiece domain are  $500 \mu\text{m} \times 500 \mu\text{m}$  and meshing is done with element size of  $10 \mu\text{m}$  for EDM simulation. For micro EDM process workpiece domain taken as  $100 \mu\text{m} \times 20 \mu\text{m}$ , with element size of  $1 \mu\text{m}$ .

Step 5: Choice of element: Two-dimensional, 4 Node Quadrilateral Element (thermal solid plane 55).

Step 6: Define material properties.

Step 7: Apply loads as per the given boundary conditions.

Step 8: Solve the current load step to get the result.

Step 9: Plot the required results from the obtained results.

Step 10: Finish.

### **3.2 MRR modelling of micro EDM for single discharge**

To calculate the MRR the cavity volume was divided into number of cylindrical disc. The coordinates of node boundary, generated by ANSYS, are used to calculate crater volume. The spark-off time is  $200 \mu\text{s}$ .

Total crater volume  $C_v$  given by,

$$C_v = \sum_{i=0}^n V_i$$

Where  $V_i$  is the volume of disc, given by,

$$V_i = \pi (x_i - x_0)^2 (y_i - y_{i-1})$$

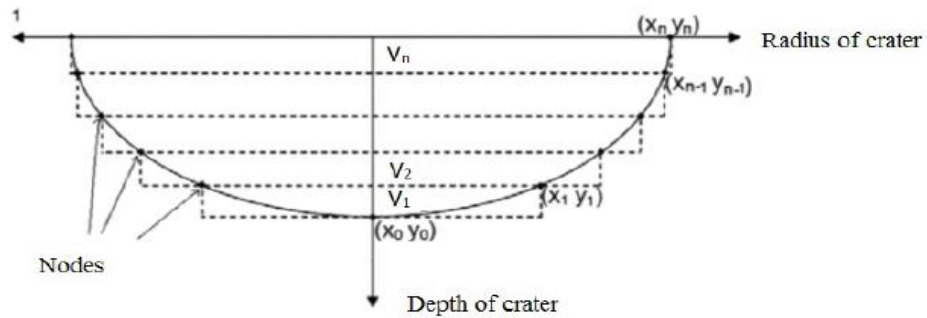


**Figure 4 Crater volume calculation**

Where  $x$  and  $y$  are the coordinates of the node and  $n$  is number of nodes.

The MRR ( $\text{mm}^3/\text{min}$ ) is computed by,

$$\text{MRR} = \frac{60 \times C_v}{(T_{on} + T_{off}) \times 10^3}$$

### 3.3 MRR calculation of micro EDM for multi-discharge

For multi-discharge analysis firstly we have to found out the number of pulses.

$$\text{NOP} = \frac{T_{machining}}{(T_{on} + T_{off})}$$

$$(\text{MRR})_{\text{multi-discharge}} = \text{NOP} \times (\text{MRR})_{\text{single-discharge}}$$

### 3.4 Residual Stress Analysis

Residual stresses or locked-in stresses can be defined as those stresses existing within a body in the absence of external loading or thermal gradients. In other words residual stresses in a structural material or component are those stresses which exist in the object without the application of any service or other external loads. Residual stresses are known to influence a material's mechanical properties such as creep or fatigue life. Sometimes, the effect on properties is beneficial; other times, the effect is very deleterious. Therefore, it is important to be able to monitor and control the residual stresses. Allen et al. [38] presented process simulation and residual stress analysis for the micro-EDM machining on molybdenum. Material removal is analysed using a thermo-numerical model, which simulates a single spark discharge process.

Using the numerical model, the effects of important EDM parameters such as the pulse duration on the crater dimension and the tool wear percentage were studied. Das et al. [111] presented a finite element-based model for the electric discharge machining (EDM) process. The model uses process parameters such as power input, pulse duration, etc., to predict the transient temperature distribution, liquid- and solid-state material transformation, and residual stresses that are induced in the workpiece as a result of a single-pulse discharge.

#### 3.4.1 Coupled thermal-structural finite element simulation of the micro-EDM process

Material is removed due to thermal action of the micro EDM process hence residual stresses are developed in the workpiece affecting its surface integrity. Small surface cracks and stress corrosion cracking may appear as a result, which will reduce the fatigue life and corrosion performance of the components.

To determine the induced stress in the workpiece, a time dependent temperature profile due to a spark discharge has to be determined first using a transient thermal analysis. A sequentially coupled thermal-structural analysis is performed using the ANSYS 12.0. An axisymmetric model is employed with element type 'Plane 55' for the thermal analysis and 'Plane 42' for the structural analysis shown in fig. 3.

For structural analysis we are keeping displacement at boundary 3 and 4 to 0 for all degree offreedom. Fig. 5 shows flow chart for the procedure used to obtain the thermal and residual stresses.

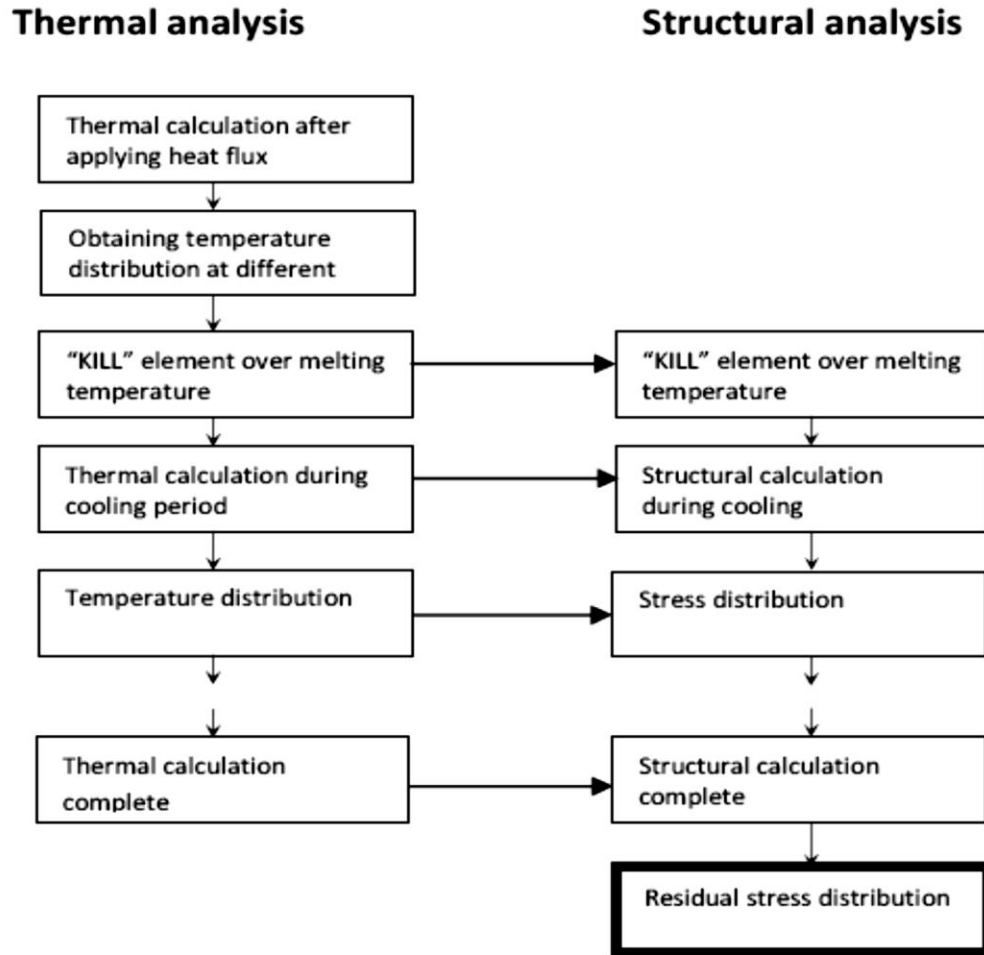


Figure 5 Flow chart for the procedure used to obtain the thermal and residual stresses

### 3.4.2 Modelling procedure using ANSYS

EDM is a complicated process that requires a powerful tool to simulate the process. In present analysis the simulation has been done on ANSYS 12.0 multi-physics. Analysis of any complex geometry can be easily done using ANSYS. It has many finite element analysis capabilities,

ranging from a simple, linear, static analysis to a complex, nonlinear, transient dynamic analysis in the fields such as structural mechanics, thermal systems, fluid mechanics, and electromagnetic.

For micro EDM analysis the geometry size taken as  $100\ \mu\text{m} \times 20\ \mu\text{m}$ , with an element size of  $1\ \mu\text{m}$ . The following procedures have been followed for coupled analysis.

Step 1: Start ANSYS 12.0.

Step 2: Units: S.I.

Step 3: Analysis method: Thermal, h method

Step 4: Problem domain: In this step, the geometry of the problem is created using ANSYS. Two-dimensional workpiece geometry is created. However, the domain is axisymmetric about Y axis, dimensions of the workpiece domain are  $100\ \mu\text{m} \times 20\ \mu\text{m}$  and meshing is done with element size of  $1\ \mu\text{m}$  for micro EDM simulation.

Step 5: Choice of element: Two-dimensional, 4 Noded Quadrilateral Element (thermal solid plane 55).

Step 6: Define material properties.

Step 7: Apply loads as per the given boundary conditions.

Step 8: Solve the current load step to get the result.

Step 9: Kill element above melting temperature of workpiece.

Step 10: Switch to structural analysis.

Step 11: Apply structural boundary conditions.

Step 12: Transfer thermal load data to structural problem.

Step 13: Plot the required results from the obtained results.

Step 14: Finish.

# Chapter 4

**EXPERIMENTAL DETAILS**

## 4 Experimental Details

- ✓  $L_4$  orthogonal array has been adopted to design the experiment. The experimental design has 2 level and 3 factors.
- ✓ Process parameters have been optimized by Grey-based Taguchi method.
- ✓ Experiment has been performed on AGIE 250c.
- ✓ Optical microscope has been used to capture the images of drilled hole.
- ✓ Dimensions of the holes were measured by using Calipro software.
- ✓ Modeling of micro EDM processes were performed by ANSYS 12.0, parameter has been optimized by  $L_9$  OA.



**Figure 6 AGIE 250c**

#### 4.1 Specifications of AGIE250c

Dielectric used	EDM30
Resolution	0.001mm
Max. workpiece size	100×700×320mm
Max. travel	700×500×500mm
Manufacture	AGIE, Switzerland

**Table 4 Process parameters used for experiment**

Parameters	Units	Value
Voltage	V	2, 6
Current	I	3, 5
Pulse-on time	μs	2, 4

**Table 5 Taguchi's L4 orthogonal array**

S. No.	Voltage (V)	Current (A)	T <sub>on</sub> (μs)
1	2	3	2
2	2	5	4
3	6	3	4
4	6	5	2



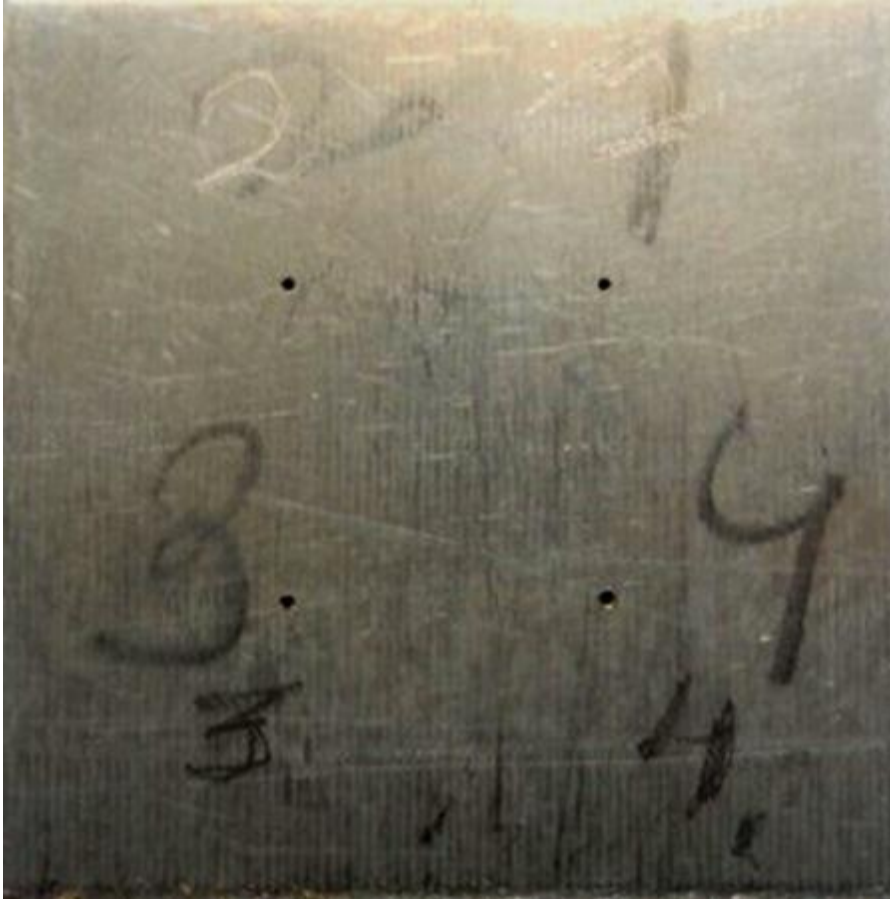


**Figure 7 Test specimen**

The Figure 6 shows the Inconel test specimen with dimensions of  $29.4 \times 29.4$ mm and thickness of 0.95mm. The holes were drilled with different parameter setting as given in Table 5, numbered as 1, 2, 3 and 4. The workpiece were examined under optical microscope with zoom level of  $45\times$  and under SEM with zoom level of  $200\times$ . Different performance characteristics were examined.

## **4.2 Taguchi method**

Taguchi's philosophy is an efficient tool for the design of high quality manufacturing system; it is based on OA experiments, which provides much-reduced variance for the experiment with optimum setting of process control parameters. Taguchi method uses a statistical measure of performance called signal-to-noise ratio. The S/N ratio takes both the mean and the variability into account. The S/N ratio is the ratio of the mean (signal) to the standard deviation (noise). The standard S/N ratios generally used are as follows: Nominal is best (NB), lower the better (LB)

and higher the better (HB). The optimal setting is the parameter combination, which has the highest S/N ratio.

In this analysis we deal with the analysis of the experiment by the Taguchi methodology, Taguchi analysis consists of the orthogonal arrays. L<sub>4</sub> and L<sub>9</sub> orthogonal arrays (OA) have been used to determine the importance of the factors or the parameters.

For the experimental work our main responses are:

- Machining time
- Circularity error
- Burr size
- Overcut

For optimization of FEA model our main responses are:

- MRR
- Residual stress

### 4.3 Grey relational analysis

Taguchi alone cannot solve multi-objective problems. Grey relational analysis is used to convert a multi-objective problem into a single objective problem.

Step 1. In Grey relational analysis firstly the experimental data i.e., measured quantity characteristics are normalized ranging from zero to one. This process is called as Grey relational generation. Depending upon the criteria objective function may be Lower-the-Better, Higher-the-Better or Nominal-is-Best.

For Lower-the-Better

$$X_i(k) = \frac{\max y_i(k) - y_i(k)}{\max y_i(k) - \min y_i(k)}$$

For Higher-the-Better

$$X_i(k) = \frac{y_i(k) - \min y_i(k)}{\max y_i(k) - \min y_i(k)}$$

where  $X_i(k)$  = Value after Grey relational generation

Min  $Y_i(k)$  = minimum of  $Y_i(k)$  for  $k^{\text{th}}$  Response

Max  $Y_i(k)$  = maximum of  $Y_i(k)$  for  $k^{\text{th}}$  Response

Step 2. Calculation of Grey relation Co-efficient

$$\xi_i(k) = \frac{\Delta_{\min} + \psi \Delta_{\max}}{\Delta_{0i}(k) + \psi \Delta_{\max}}$$

where  $\Delta_{0i}(k) = |x_0(k) - x_i(k)|$  = Difference between absolute Values of  $x_0(k)$  and  $x_i(k)$

Step 3. After taking average of the Grey relational coefficients, the Grey relational grade can be calculated as:

$$\gamma_i = \frac{1}{n} \sum_{k=1}^n \xi_i(k)$$

Process parameters used for modelling the micro EDM process has been shown in Table 6. For the optimization of ANSYS model parameter setting has been shown in Table 7.

**Table 6 Process parameters used for modelling (Micro EDM)**

<b>PARAMETERS</b>	<b>Micro EDM (LEVELS)</b>		
Voltage	20V	25V	30V
Current	1.5A	3A	5A
Heat input to the workpiece	.08	0.15	0.2
Spark radius	5 $\mu$ m		
Pulse-on time	2 $\mu$ s		
Pulse-off time	100 $\mu$ s		

**Table 7 Taguchi L9 Array of process parameters for Micro EDM**

<b>S. No.</b>	<b>VOLTAGE</b>	<b>CURRENT</b>	<b>HEAT INPUT</b>
<b>1</b>	20	1.5	0.08
<b>2</b>	20	3.0	0.15
<b>3</b>	20	5.0	0.20
<b>4</b>	25	1.5	0.15
<b>5</b>	25	3.0	0.20
<b>6</b>	25	5.0	0.08
<b>7</b>	30	1.5	0.20
<b>8</b>	30	3.0	0.08
<b>9</b>	30	5.0	0.15

# Chapter 5

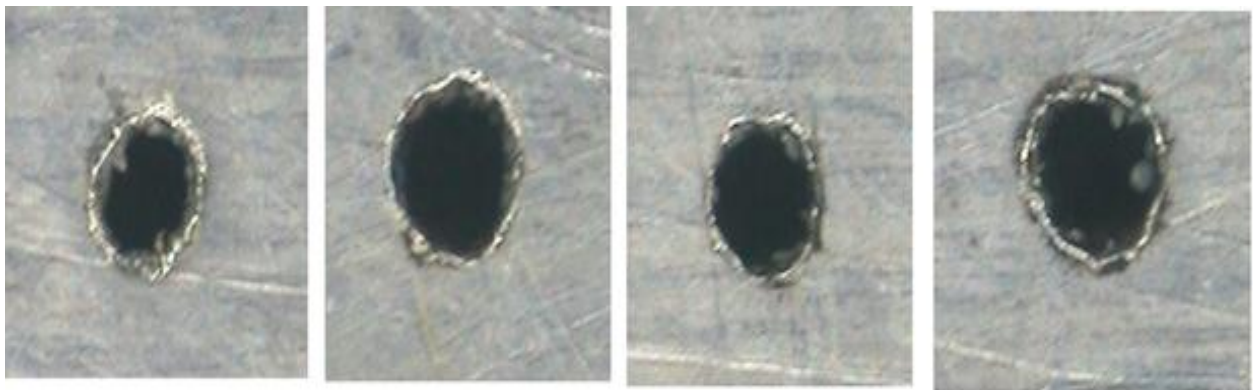
## RESULTS AND DISCUSSIONS

## 5. Results and discussion

### 5.1. Optimization of micro EDM

Four holes were drilled according to design shown in Table 5 with process parameter setting as shown in Table 4. From the four holes one can see the white colours disturbances around the circumference of the holes produced and that white coloured disturbance is nothing but the hard layer which is called as the recast layer which always formed around the micro-EDMed holes. Recast layer is defined as a layer forms on the workpiece surface defined as a recast layer after solidification. Moulds and dies desire to remove the RCL even though it is hard and has good matrix adherence. This is formed due to sparks whose thermal energy melts the metal and then that melted metal undergoes rapid quenching to form recast layer.

The main responses in present analysis are machining time, burr size, overcut, and circularity error. The optimization criteria for all the response are Lower-the-Better.



(A)

(B)

(C)

(D)

**Figure 8 Drilled micro holes on Inconel 718 with different parameter settings**

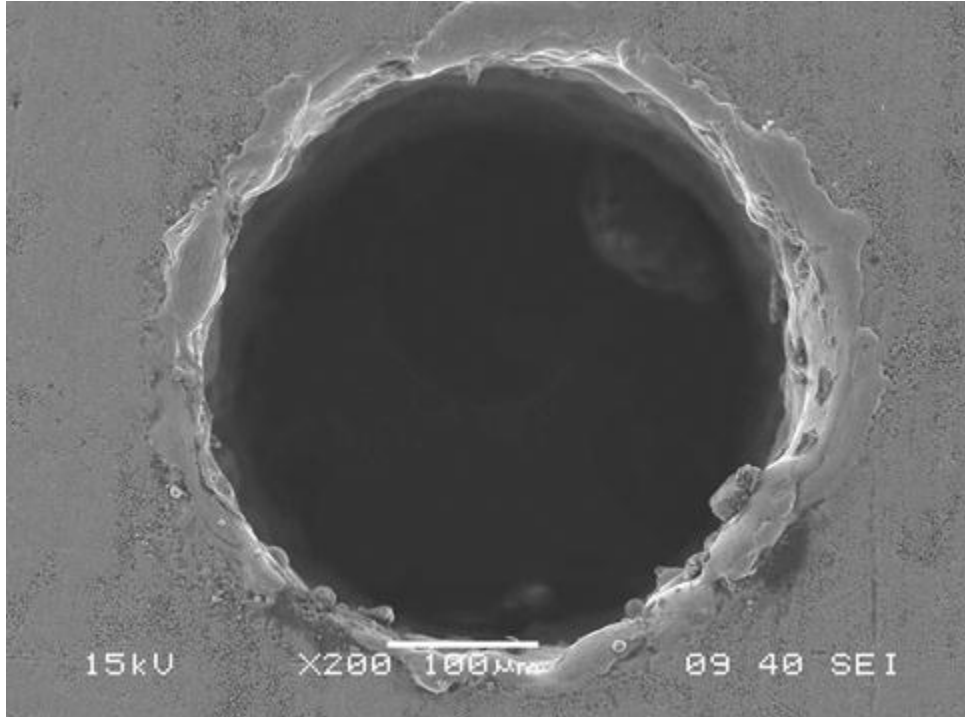


**Figure 9 SEM image of micro hole at  $V = 2V$ ,  $I = 3A$  and  $T_{on} = 2\mu s$**

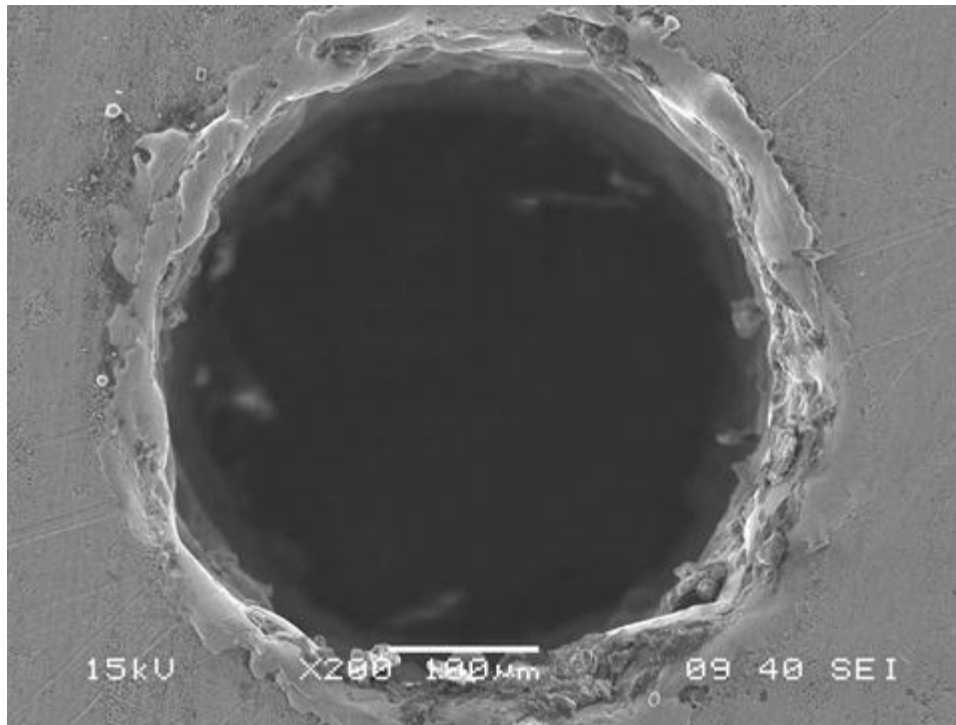


**Figure 10 SEM image of micro hole at  $V = 2V$ ,  $I = 5A$  and  $T_{on} = 4\mu s$**

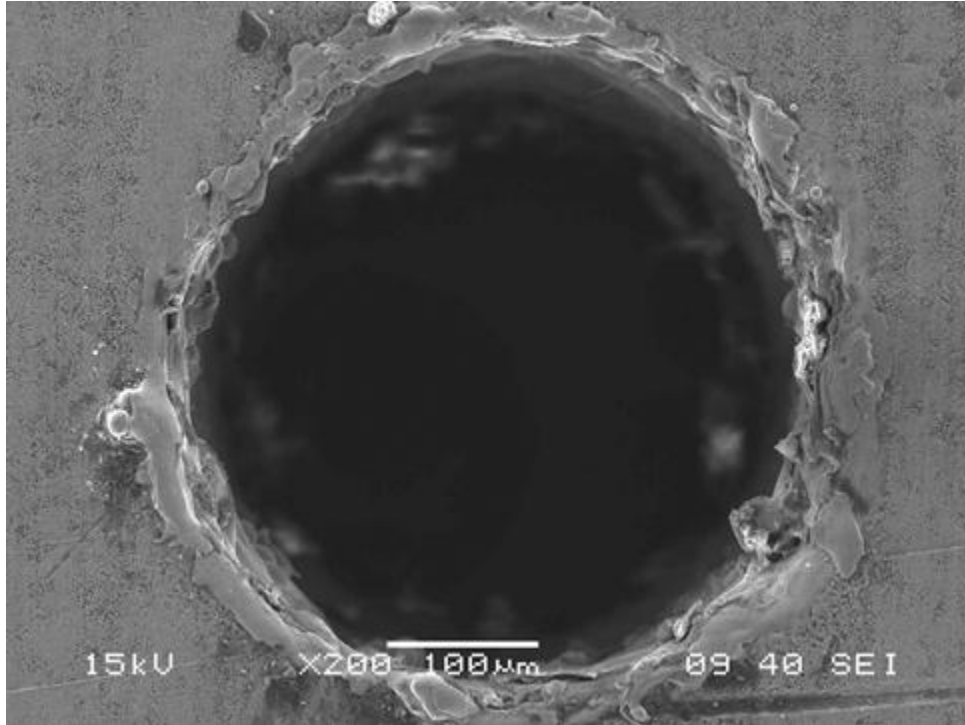


**Figure 11 SEM image of micro hole at  $V = 6V$ ,  $I = 3A$  and  $T_{on} = 4\mu s$**

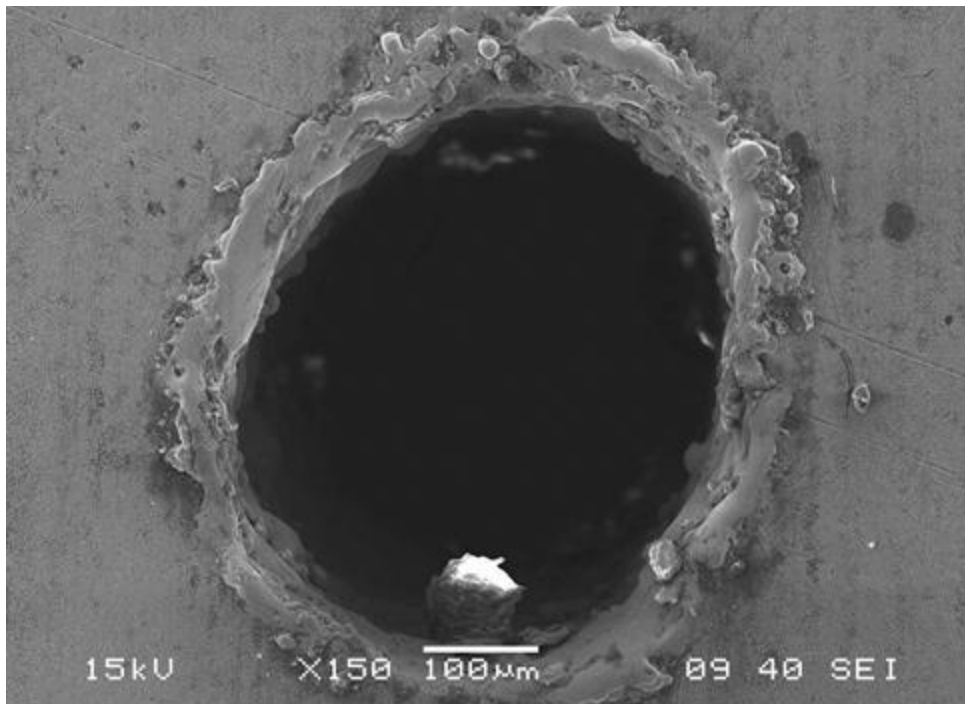


**Figure 12 SEM image of micro hole at  $V = 6V$ ,  $I = 5A$  and  $T_{on} = 2\mu s$**



**Table 9 Grey relational generation**

<b>Machining time (min)</b>	<b>Overcut (<math>\mu\text{m}</math>)</b>	<b>Circularity (<math>\mu\text{m}</math>)</b>	<b>Burr size (<math>\mu\text{m}</math>)</b>
0	1	0	0.654
0.5323	0.6166	1	0.6298
1	0.5270	0.1457	1
0.9354	0	0.3589	0

**Table 10 Grey relational coefficient of each performance characteristics (with  $\psi=0.5$ )**

<b>Machining time (min)</b>	<b>Overcut (<math>\mu\text{m}</math>)</b>	<b>Circularity (<math>\mu\text{m}</math>)</b>	<b>Burr size (<math>\mu\text{m}</math>)</b>	<b>Overall grey coeff.</b>
0.3333	1	.3333	0.5910	0.5644
0.5167	0.5660	1	0.5746	0.6643
1	0.5139	0.3692	1	0.7208
0.8856	0.3333	0.4382	0.3333	0.4976

**Table 11 Response table (mean) for overall Grey relational grade**

<b>Parameters</b>	<b>Levels</b>		<b>Delta</b>
	1	2	
Voltage	0.6144	0.6092	.0052
Current	0.6426	0.5809	0.0617
Pulse-on time	0.531	0.6926	0.1616

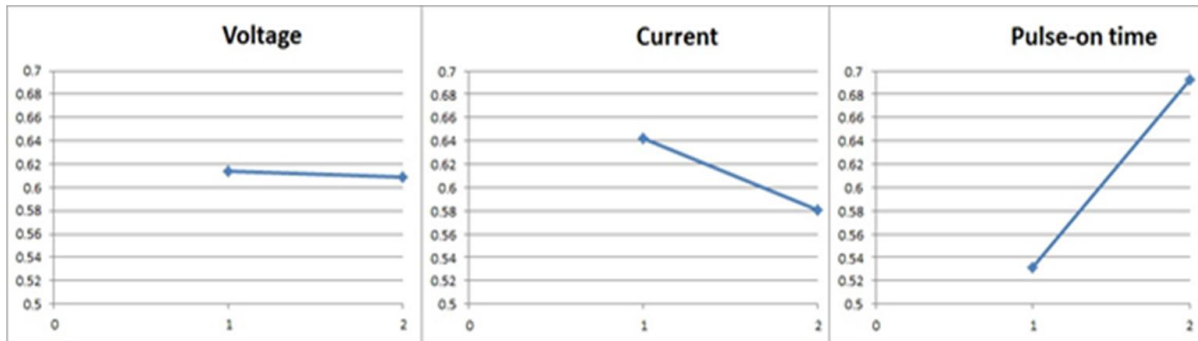


Figure 13 S/N ratio plot for overall grey relational grade

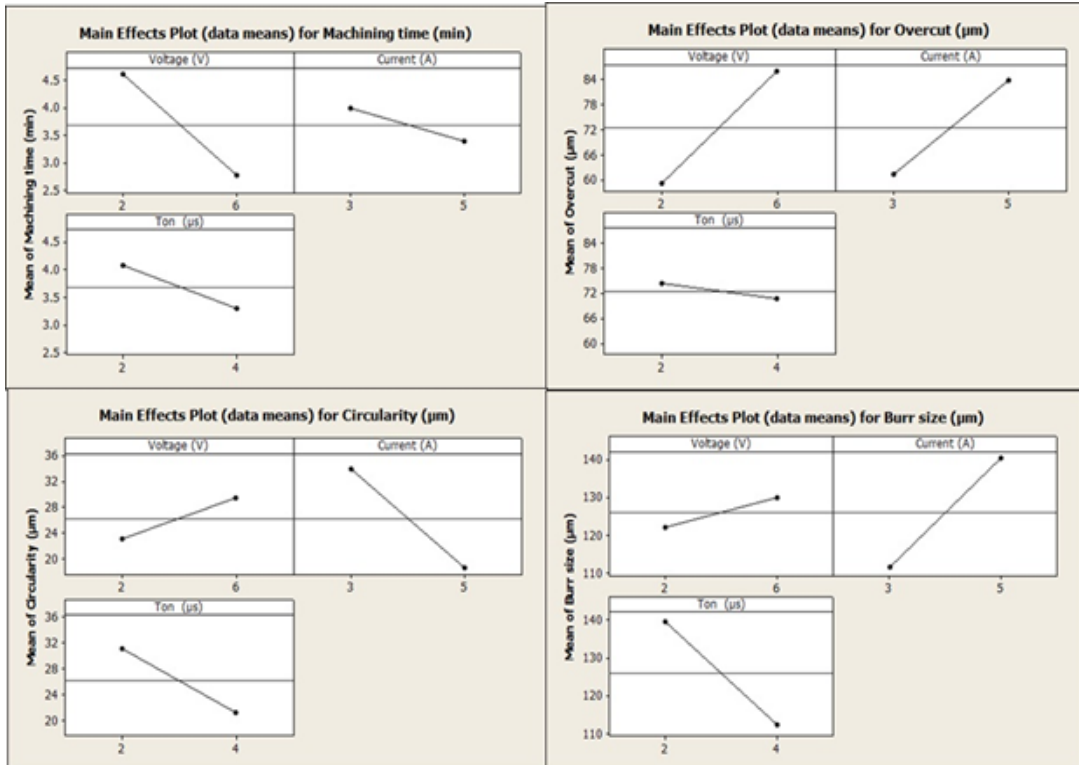


Figure 14 Main effect plots

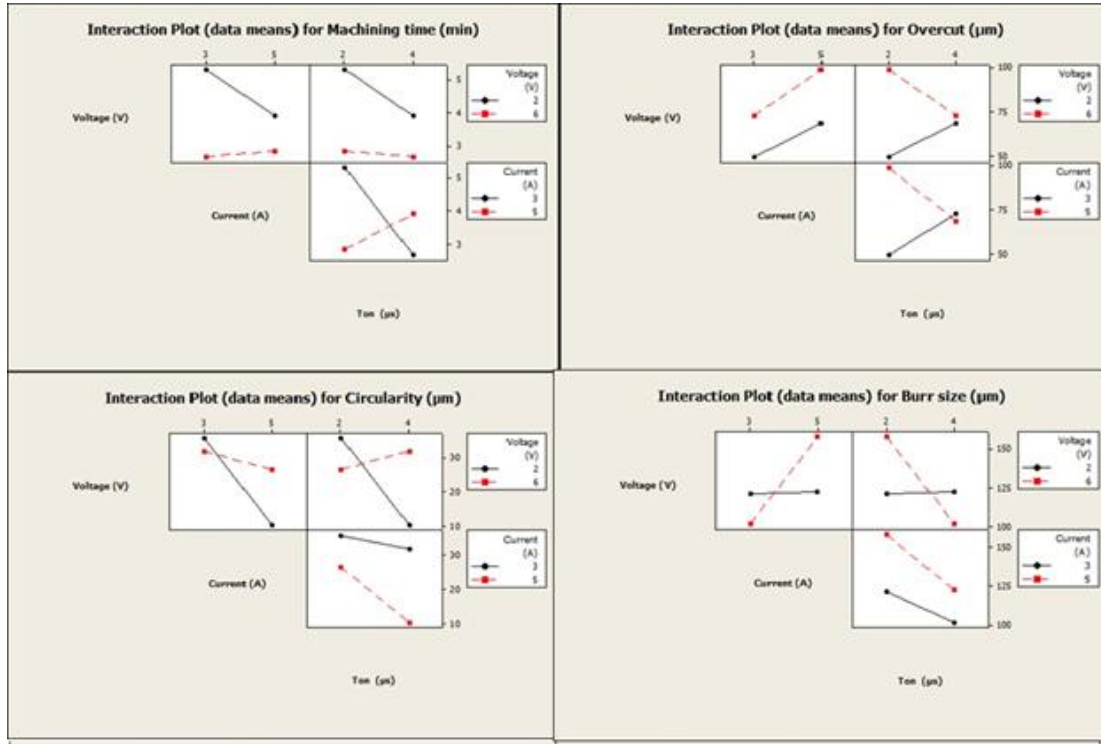


Figure 15 Interaction plot

### 5.2 ANSYS model validation

Firstly we have developed a model of EDM process for 5 Cr die steel with parameter setting as given in Table 12. Later the value has been compared with Shankar et al [p8]. Fig. 12 shows the plot for EDM process done for the 5 Cr die steel. As element size is 10 µm so we are getting a distance of 40 µm at node 6 as shown in Fig. 3, the temperature at node 6 is coming 2942K, which is approximately same as given by Shankar et al [8]. So we can say that we are proceeding in the right way. Further in the analysis the EDM problem is extended to the micro EDM. For micro EDM the parameter setting is given in Table 6.

**Table 12 EDM process parameters**

Parameters	Units	Value
Discharge voltage	V	28
Current	A	6.5
Percentage of heat input to the workpiece		0.42
Spark radius	$\mu\text{m}$	115
Pulse-on time	$\mu\text{s}$	60
Heat transfer coefficient	$\text{W}/\text{m}^2\text{k}$	10,000

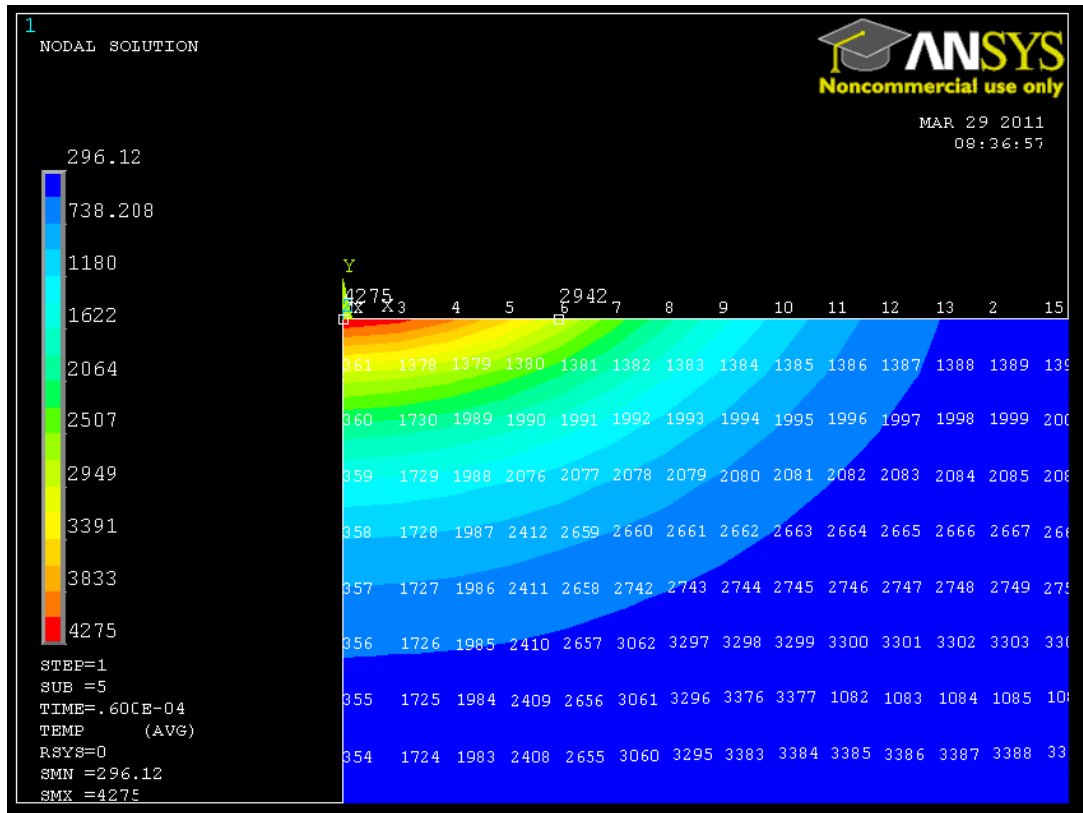


**Figure 16 Nodal temperature distribution in 5 Cr die steel for EDM process**

### 5.3 MRR modelling of micro EDM for single discharge

After validating the model MRR for micro EDM process, with different process parameter setting as given in Table 7, have been calculated.

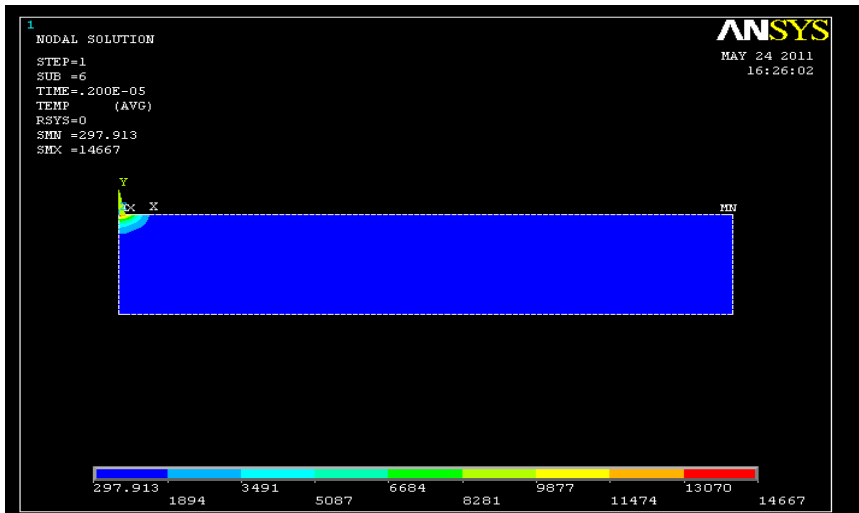


Figure 17 Temperature distribution in Inconel 718 with V=20V, I=1.5A and P=0.08

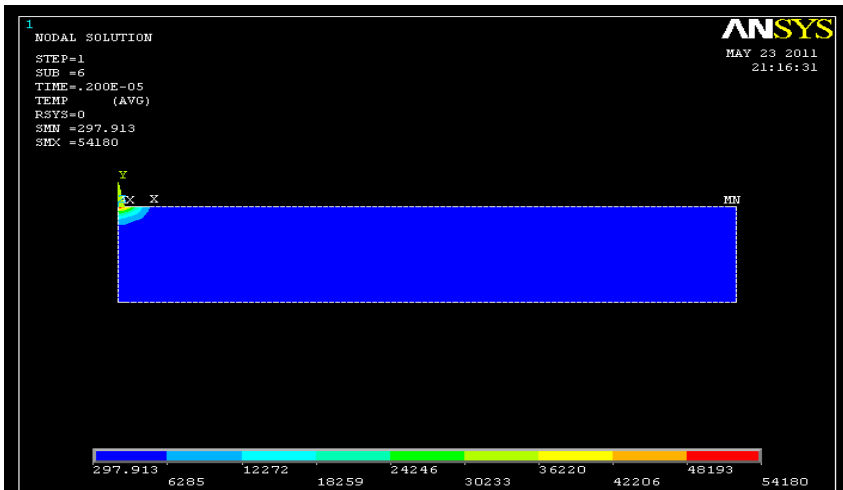


Figure 18 Temperature distribution in Inconel 718 with V=20V, I=3A and P=0.15

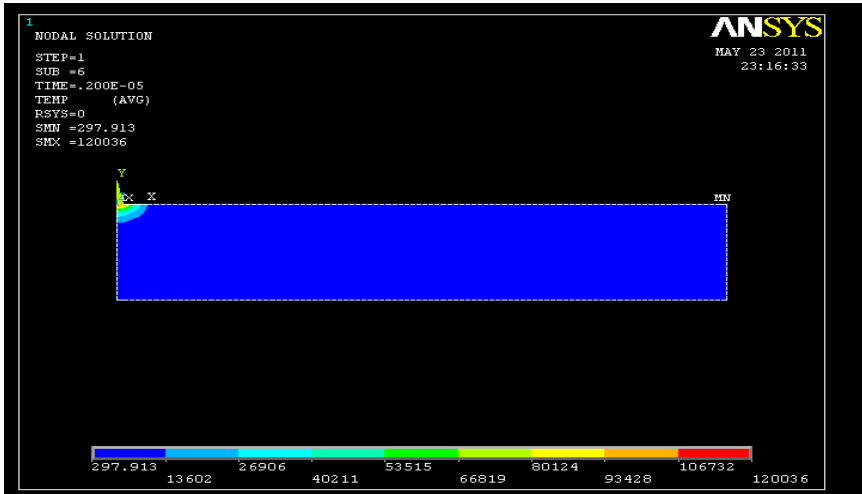


Figure 19 Temperature distribution in Inconel 718 with  $V=20V$ ,  $I=5A$  and  $P=0.20$

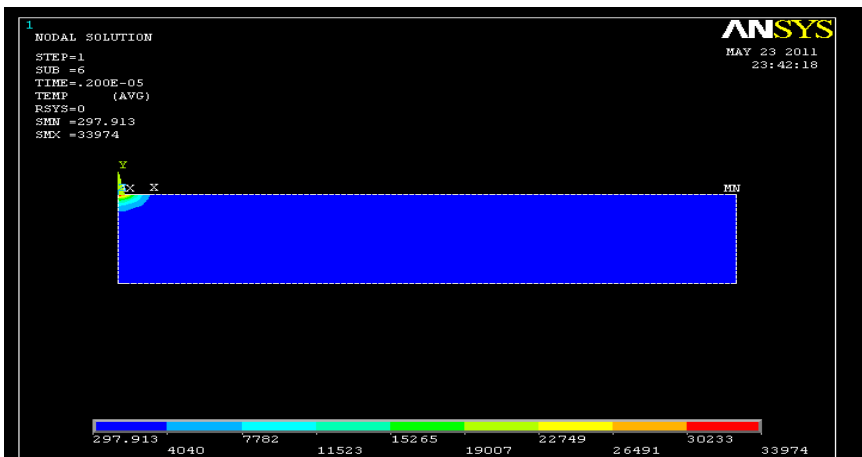


Figure 20 Temperature distribution in Inconel 718 with  $V=25V$ ,  $I=1.5A$  and  $P=0.15$

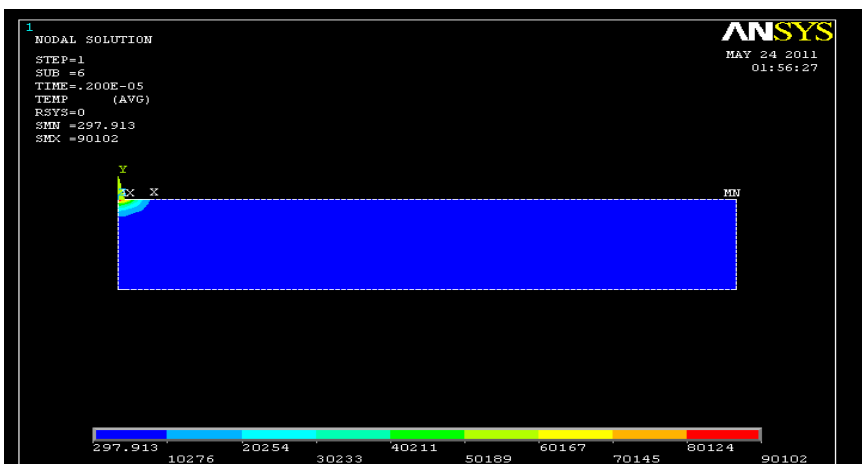


Figure 21 Temperature distribution in Inconel 718 with  $V=25V$ ,  $I=3A$  and  $P=0.20$

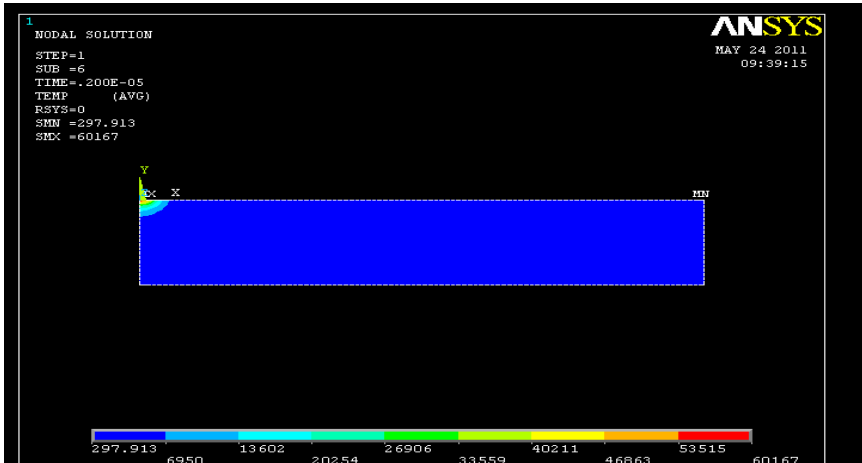


Figure 22 Temperature distribution in Inconel 718 with  $V=25V$ ,  $I=5A$  and  $P=0.08$

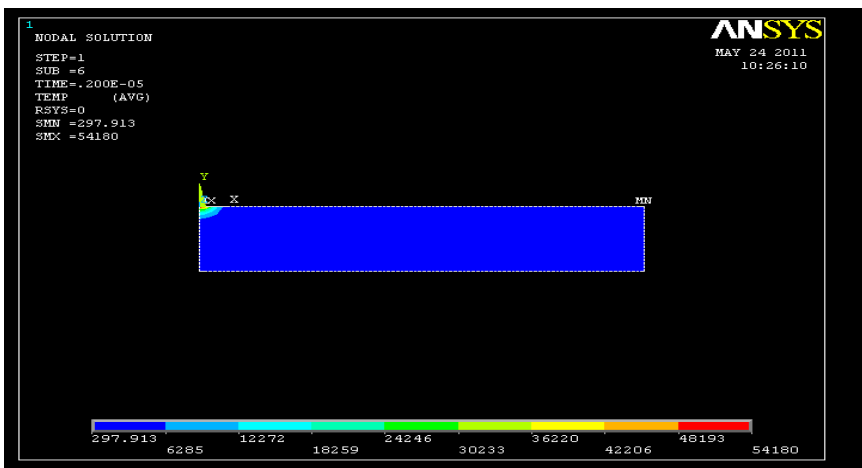


Figure 23 Temperature distribution in Inconel 718 with  $V=30V$ ,  $I=1.5A$  and  $P=0.20$

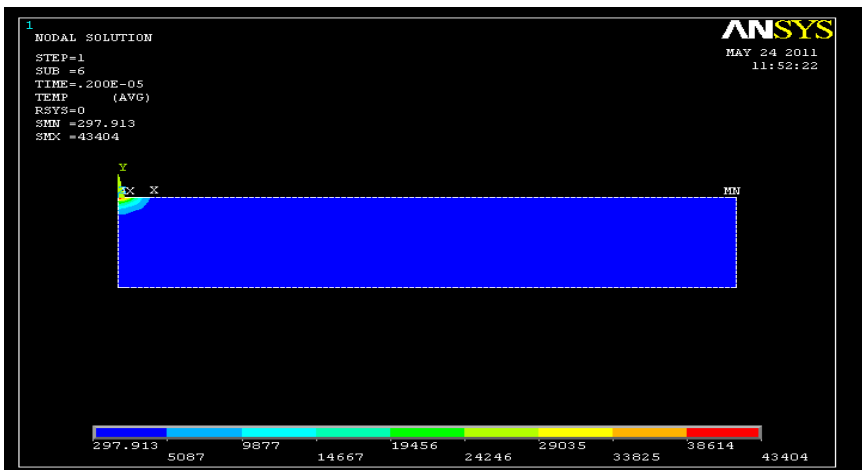
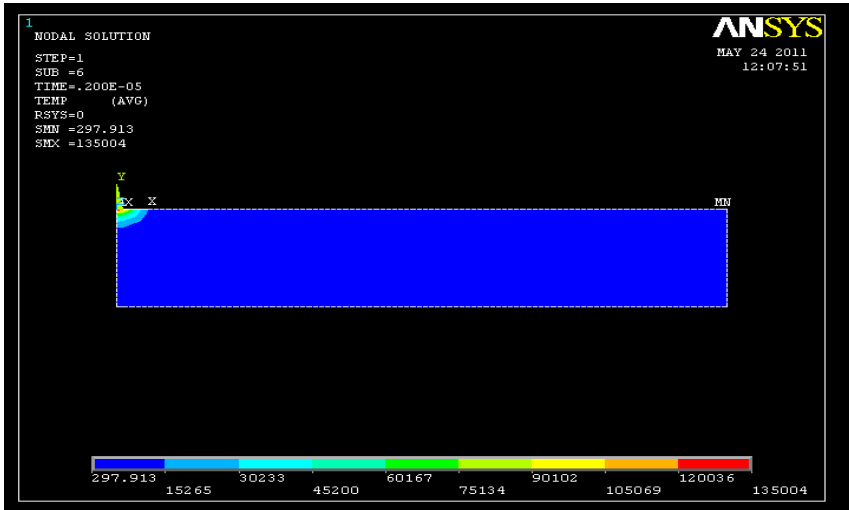


Figure 24 Temperature distribution in Inconel 718 with  $V=30V$ ,  $I=3A$  and  $P=0.08$



**Figure 25 Temperature distribution in Inconel 718 with  $V=30V$ ,  $I=5A$  and  $P=0.15$**

After getting the temperature distribution for different process parameters, the elements whose temperature rose above the melting point using “KILL” element.

#### 5.4 Residual stress analysis

Electrical discharge machining causes thermally induced residual tensile stress to form in the top layer of a machined surface. The state of residual stress influences the fatigue behaviour, dimensional stability and possible stress corrosion of a machined component.

Residual stresses are self-equilibrating stresses that exist in a body if all external loads are removed. They occur when a body is subjected to non-uniform plastic deformations or changes of specific volume.



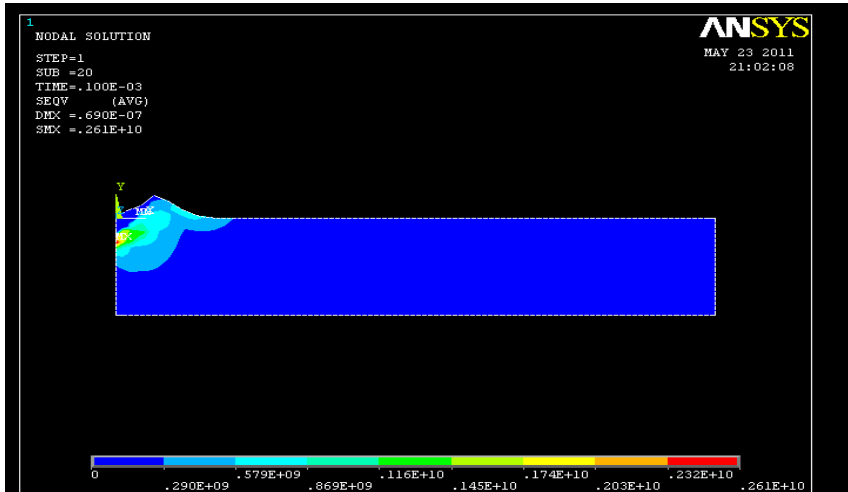


Figure 26 Residual stress distribution in Inconel 718 with V=20V, I=1.5A and P=0.08

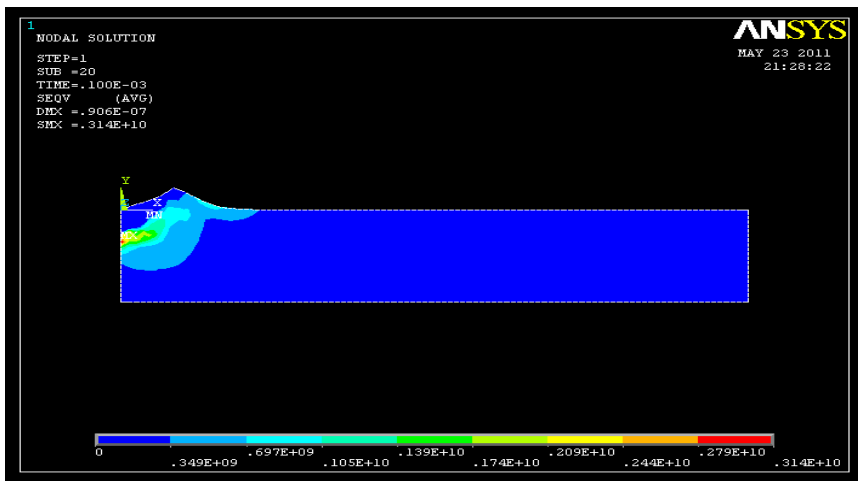


Figure 27 . Residual stress distribution in Inconel 718 with V=20V, I=3A and P=0.15

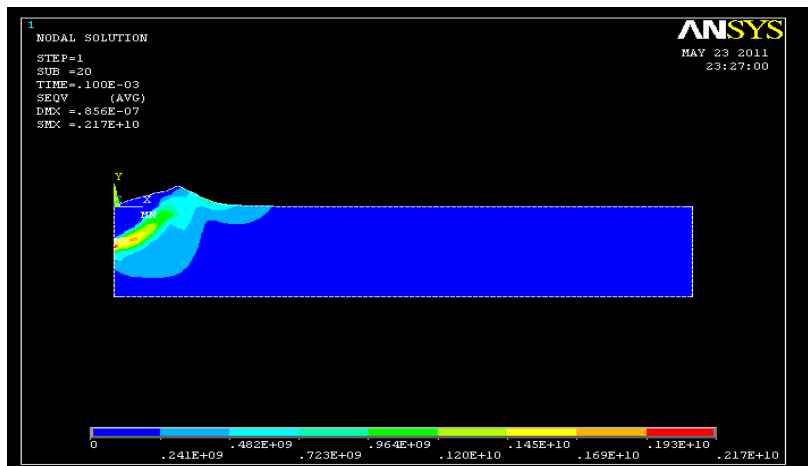


Figure 28 Residual stress distribution in Inconel 718 with V=20V, I=5A and P=0.2

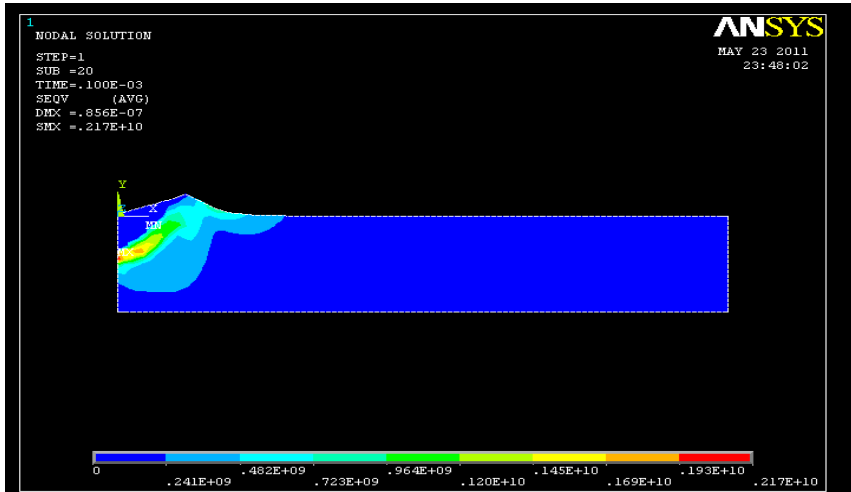


Figure 29 Residual stress distribution in Inconel 718 with V=25V, I=1.5A and P=0.15

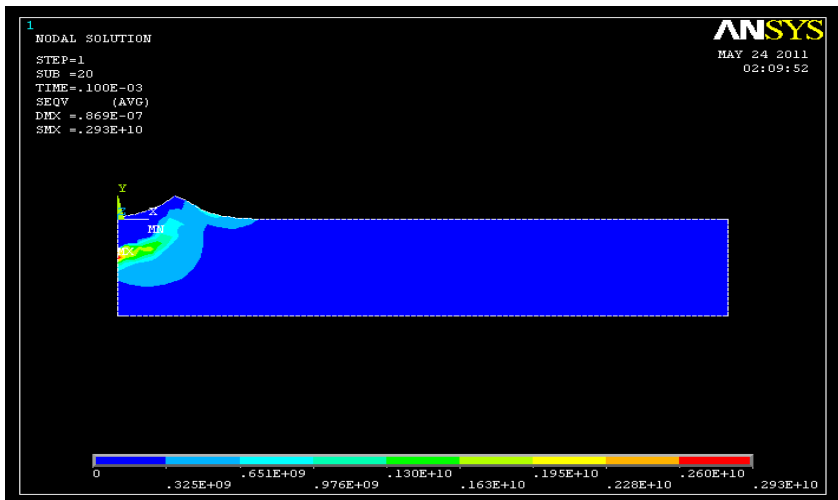


Figure 30 Residual stress distribution in Inconel 718 with V=25V, I=3A and P=0.2

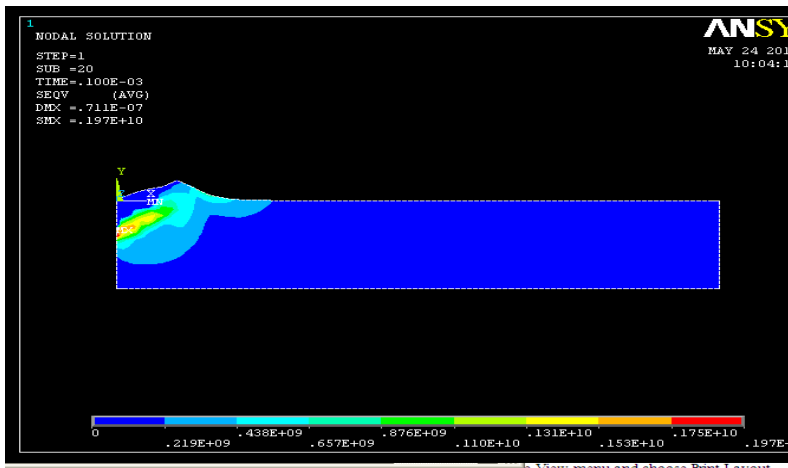


Figure 31 Residual stress distribution in Inconel 718 with V=25V, I=5A and P=0.08

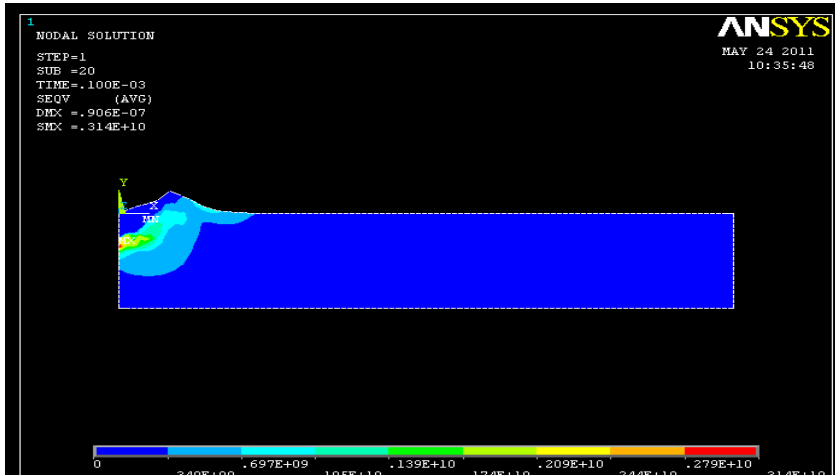


Figure 32 Residual stress distribution in Inconel 718 with V=30V, I=1.5A and P=0.2

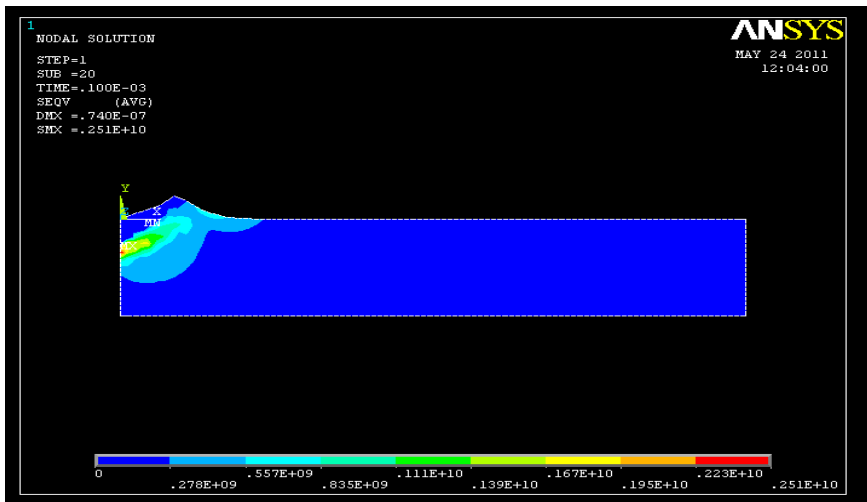


Figure 33 Residual stress distribution in Inconel 718 with V=30V, I=3A and P=0.08

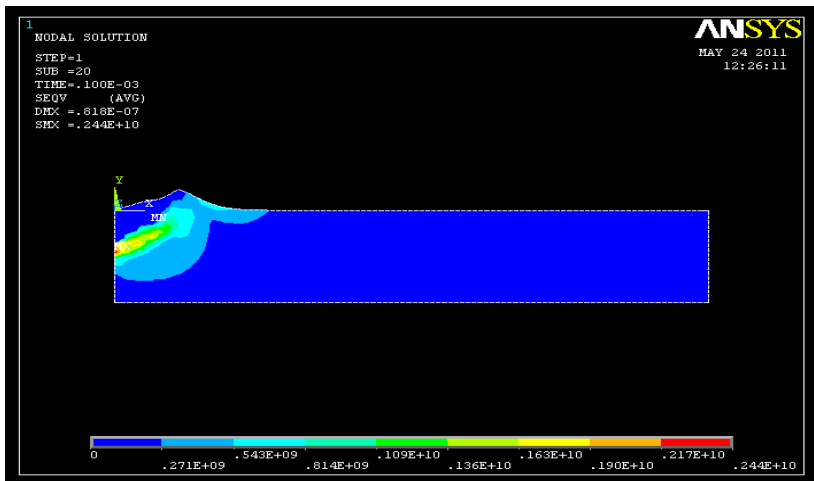


Figure 34 Residual stress distribution in Inconel 718 with V=30V, I=5A and P=0.15

### 5.5 Optimization of model for micro EDM process

The modelling of micro EDM process has been done using ANSYS 12.0. The main responses for the model are MRR and residual stress, for MRR Higher-the-Better and for residual stress lower-the-Better criteria is to be adopted.

**Table 13 Experimental data obtain from model of micro EDM**

<b>S. No.</b>	<b>VOLTAGE</b>	<b>CURRENT</b>	<b>HEAT INPUT</b>	<b>MRR (mm<sup>3</sup>/min)</b>	<b>Residual stress (GPa)</b>
<b>1</b>	20	1.5	0.08	138599.412	2.61
<b>2</b>	20	3.0	0.15	413950.588	3.14
<b>3</b>	20	5.0	0.20	755830	2.17
<b>4</b>	25	1.5	0.15	306767.059	2.17
<b>5</b>	25	3.0	0.20	632014.118	2.93
<b>6</b>	25	5.0	0.08	521134.118	1.97
<b>7</b>	30	1.5	0.20	413950.588	3.14
<b>8</b>	30	3.0	0.08	401014.706	2.51
<b>9</b>	30	5.0	0.15	838990	2.44

**Table 14 Grey relational generation and Grey relational coefficient of each performance characteristics (with  $\psi=0.5$ )**

<b>S. No.</b>	<b>MRR(Grey relation generation)</b>	<b>R. Stress (Grey relation generation)</b>	<b>MRR (Grey relational coefficient , <math>\psi = 0.5</math>)</b>	<b>R. Stress (Grey relational coefficient , <math>\psi = 0.5</math>)</b>	<b>Overall grade</b>
<b>1</b>	0	0.453	0.33	0.478	0.404
<b>2</b>	0.393	0	0.452	0.333	0.3925
<b>3</b>	0.881	0.829	0.808	0.745	0.7765
<b>4</b>	0.24	0.829	0.397	0.745	0.571
<b>5</b>	0.704	0.179	0.628	0.379	0.5035
<b>6</b>	0.546	1	0.524	1	0.762
<b>7</b>	0.393	0	0.452	0.333	0.3925
<b>8</b>	0.375	0.538	0.444	0.520	0.482
<b>9</b>	1	0.598	1	0.554	0.777

**Table 15 Response table (mean) for overall Grey relational grade**

Factors	Grey relation grade			
	Level 1	Level 2	Level 3	Delta
<b>Voltage</b>	0.5243	0.6122	0.5505	0.0262
<b>Current</b>	0.4558	0.4593	0.7718	0.5160
<b>Heat input</b>	0.5493	0.5802	0.5575	0.0309

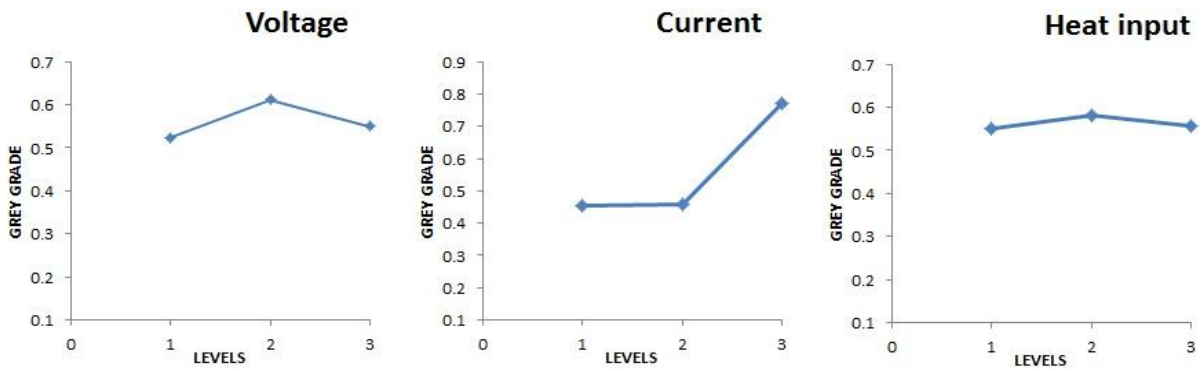


**Figure 35 S/N ratio plot For Overall Grey Relational Grade**

## 5.6 MRR modeling for multi-discharge experiment

With the parameter setting  $V=2V$   $I=3A$  and  $T_{on} = 2\mu s$  one ANSYS model has been shown in Figure 32.

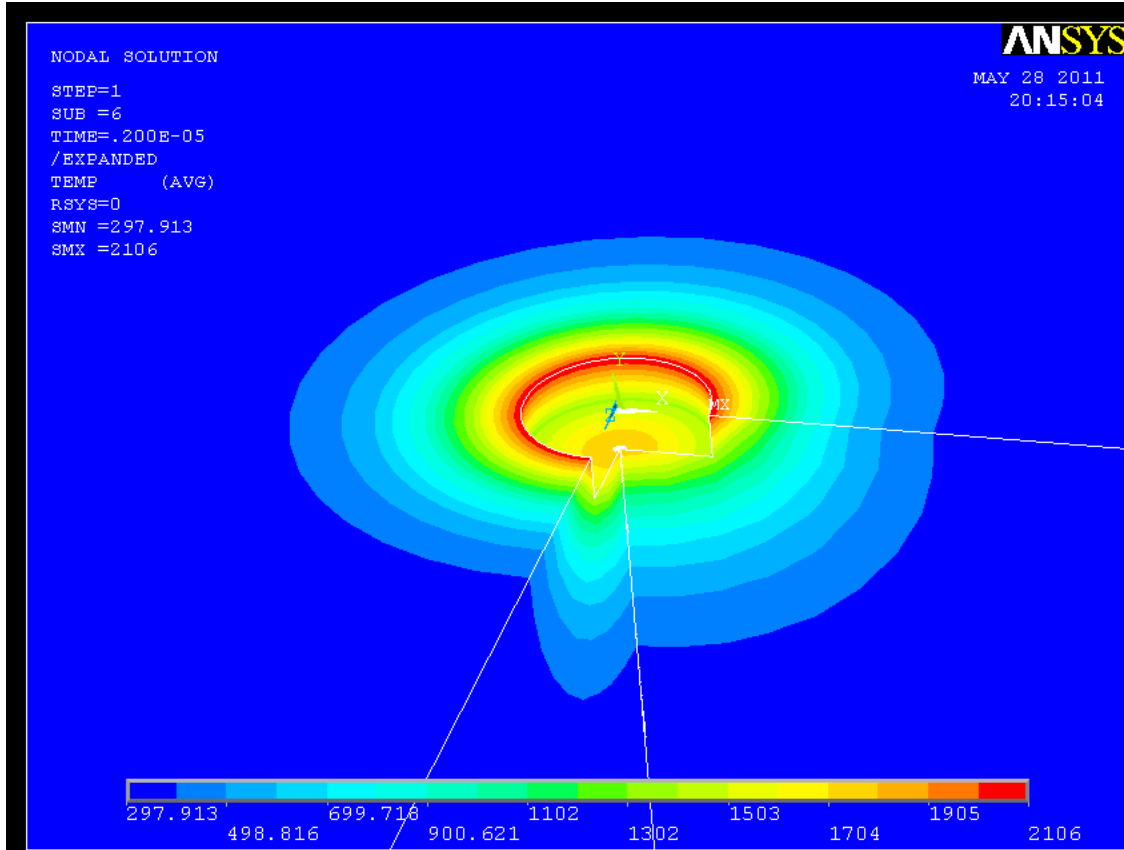


**Figure 36 Bowl shaped crater cavity at  $V=2V$ ,  $I=3A$  and  $T_{on} = 2\mu s$**

### 5.6.1 Calculation of MRR

A thermal model has been created with element size of  $0.5\mu m$  element size and  $100 \times 20 \mu m$  workpiece domain, after applying heat flux (with  $V=2V$ ,  $I=3A$  and  $T_{on} = 2\mu s$ ), and convection force, melted elements were killed and final geometry is as shown in figure 37.

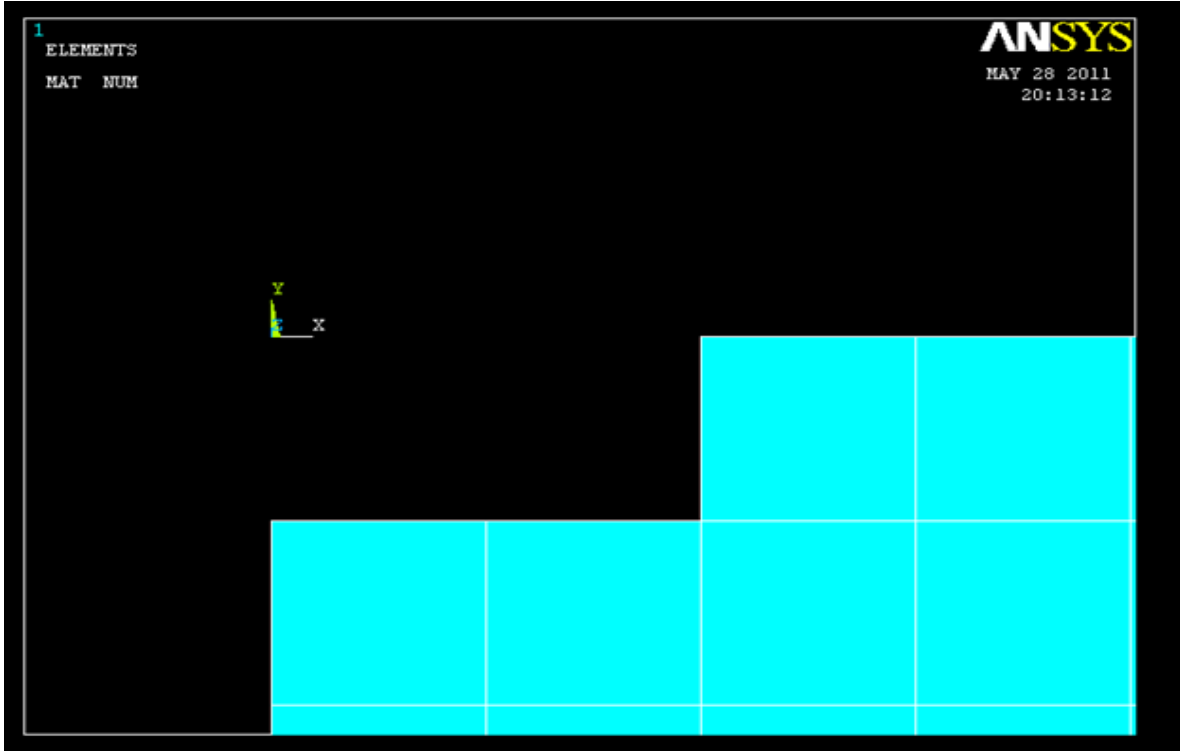


**Figure 37 Live element after application of heat flux**

To find out the MRR the element model has been divided into cylindrical disc and volume of disc is given by:

$$V_i = \pi (x_i - x_0)^2 (y_i - y_{i-1})$$

$$\begin{aligned} V_i &= \pi \times (1-0)^2 \times 0.5 \\ &= 1.57 \mu\text{m}^3 \end{aligned}$$

$$C_v = 1.57 \mu\text{m}^3$$

MRR for single discharge is given by:

$$\text{MRR} = \frac{60 \times C_v}{(T_{on} + T_{off}) \times 10^3}$$

$$\text{MRR} = 4.66 \times 10^{-4}$$

For multi-discharge ( $T_{\text{machining}} = 1\text{min}$ )



$$\text{NOP} = \frac{T_{\text{machining}}}{(T_{\text{on}} + T_{\text{off}})}$$

$$\text{NOP} = 297029.703$$

$$(\text{MRR})_{\text{multi-discharge}} = \text{NOP} \times (\text{MRR})_{\text{single-discharge}}$$

$$(\text{MRR})_{\text{multi-discharge}} = 138.416 \text{ mm}^3/\text{min}$$

From experiment  $\text{MRR} = (\text{initial weight} - \text{final weight}) / \text{machining time}$

$$\begin{aligned} &= \frac{11.847 - 11.008}{8190} \times 10^6 \\ &= 102.442 \text{ mm}^3/\text{min} \end{aligned}$$

$$\% \text{Error} = 25.98.$$

## 5.7 Effect of different process parameters

### 5.7.1 Effect of current

Fig. 38 and 39 shows the effect of current along the radius of the workpiece and along the depth respectively.

From the graph trend shown in Fig. 38 it can be observed that top surface temperature goes on increasing as we increasing the current. This is because; the heat flux equation is directly proportional to the current. Larger the current, larger the heat input hence higher the temperature.

It can be also observed that the temperature distribution follows the Gaussian distribution. Considerable temperature gradient along the radial direction can be seen up to 8  $\mu\text{m}$ . The temperature variations along the depth of workpiece are shown in Fig. 39. It can be observed that the maximum temperature is found at the top surface and decreases as we proceed downward. No considerable variation in temperature is observed after a depth of 6  $\mu\text{m}$ .

### 5.7.2 Effect of pulse duration

The effects of variation in pulse duration on surface temperature distribution are shown in Fig. 40 and 41. From the graph trend shown in Fig. 40 it can be observed that top surface temperature goes on increasing as we increasing the pulse duration. This is obvious that increase in pulse duration will increase the heat input hence increase the temperature. The temperature is

very much higher at the point of spark. Considerable temperature gradient along the radial direction can be seen up to 8  $\mu\text{m}$ .

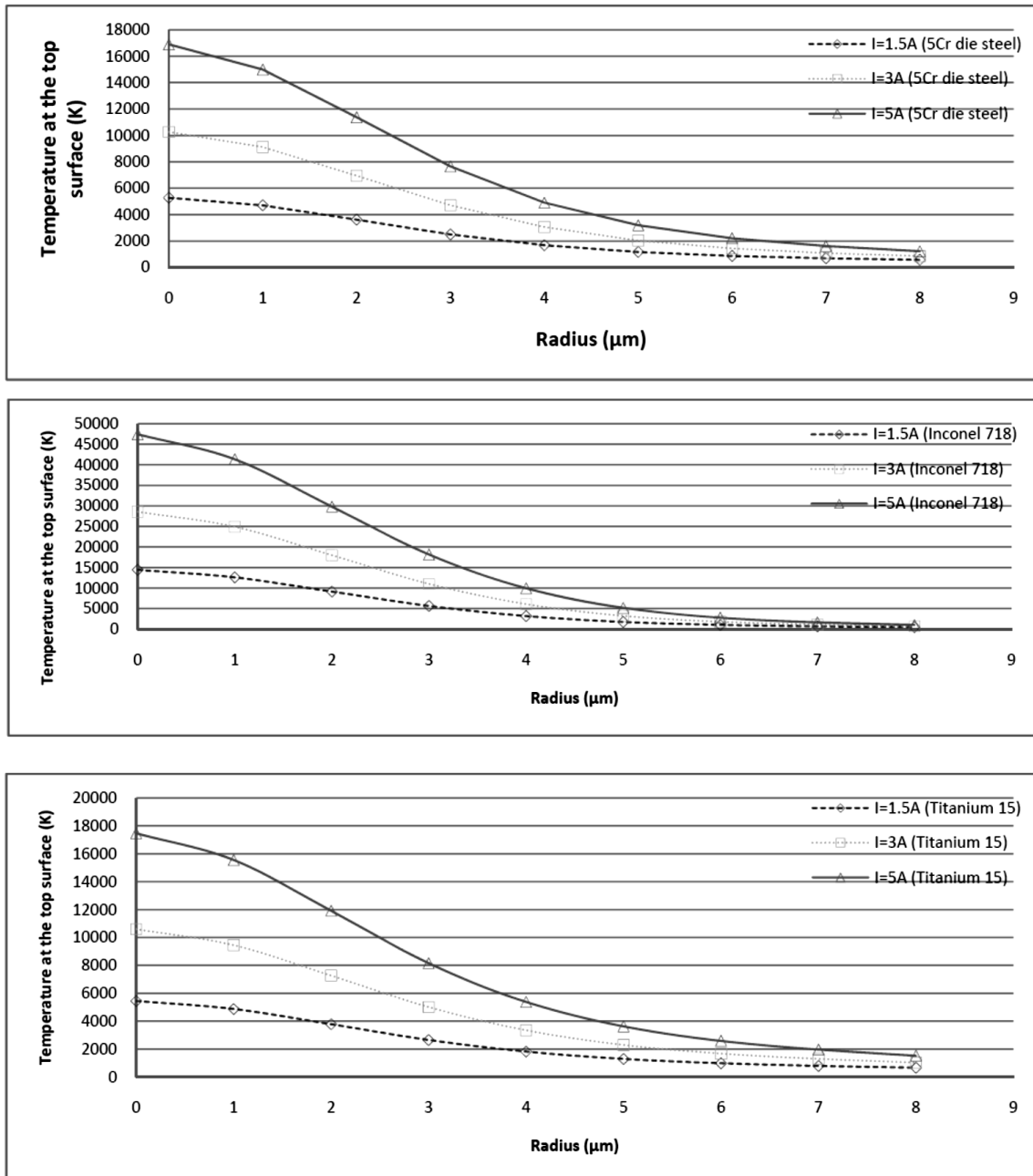
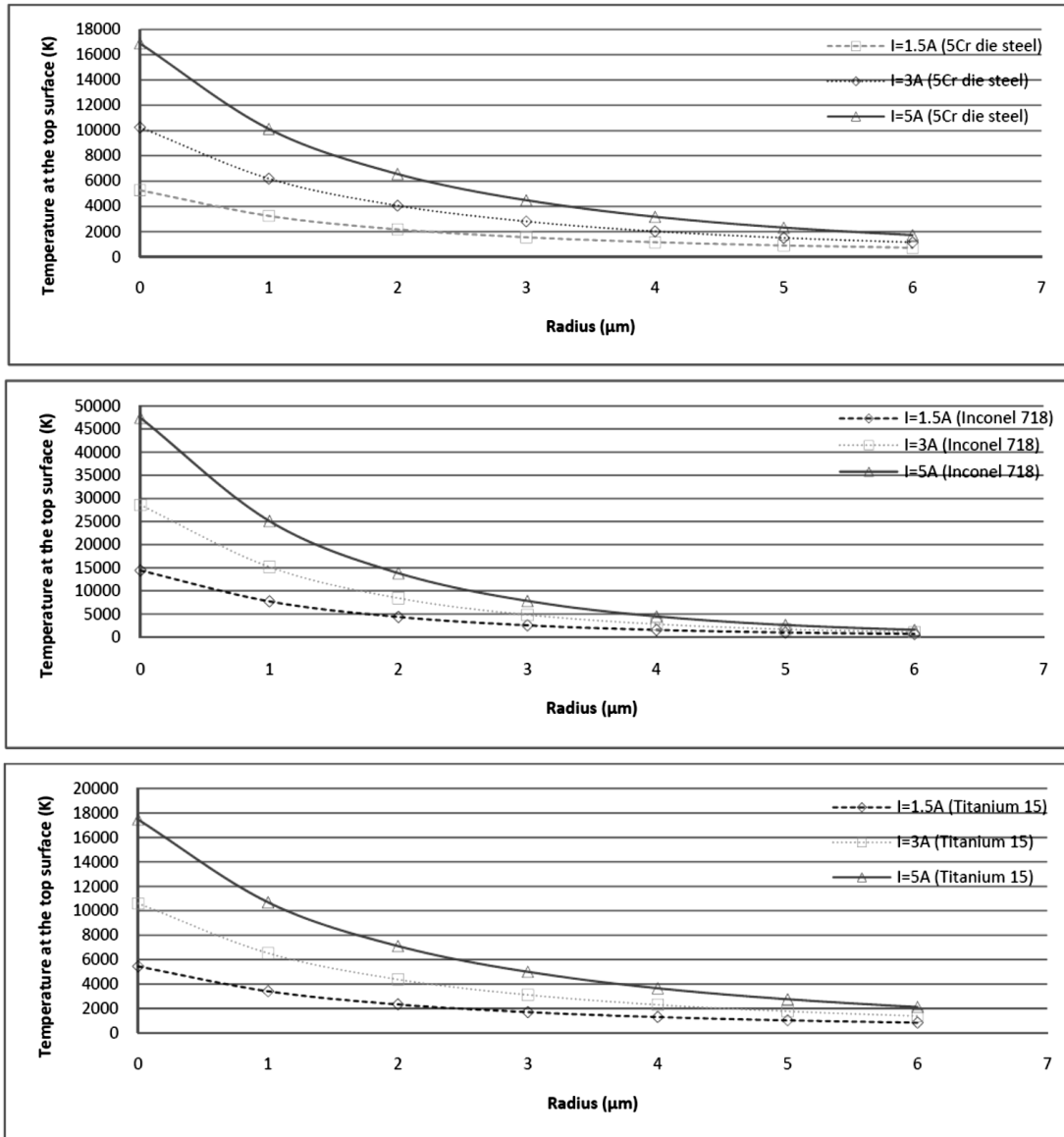


Figure 38 The effect of current on the temperature distribution along the radial direction from the centerline for micro EDM at  $P = 0.08$ ,  $T_{on} = 2 \mu\text{s}$ ,  $V = 20 \text{ V}$ .



**Figure 39** The effect of current on the temperature distribution along the depth of workpiece at the centerline for micro EDM at  $P = 0.08$ ,  $T_{on} = 2 \mu s$ ,  $V = 20 V$ .

The temperature variations along the depth of workpiece are shown in Fig. 41. It can be observed that the maximum temperature is found at the top surface and decreases as we proceed downward. No considerable variation in temperature is observed after a depth of  $8 \mu m$ , because of the convection caused by the dielectric fluid.

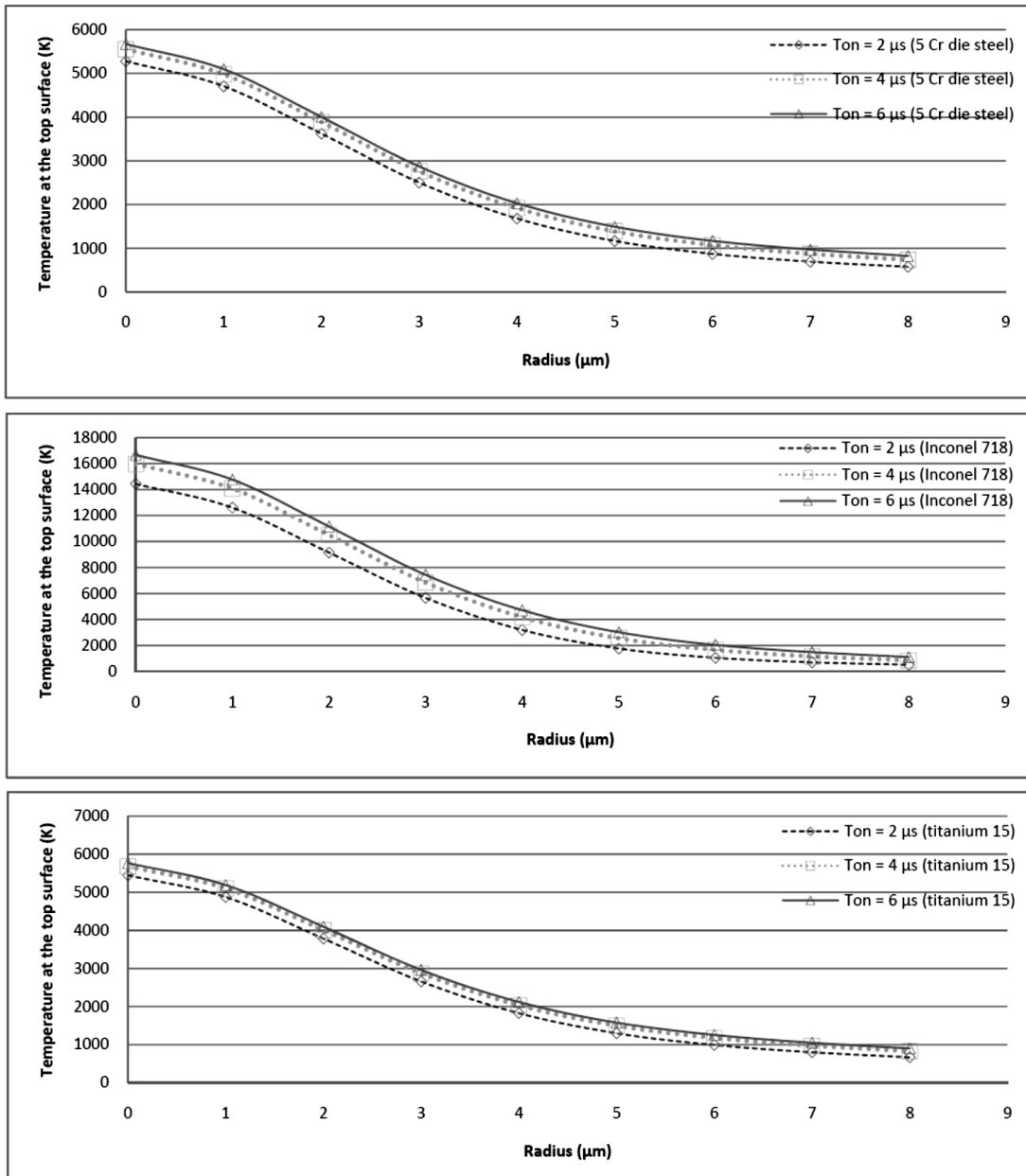
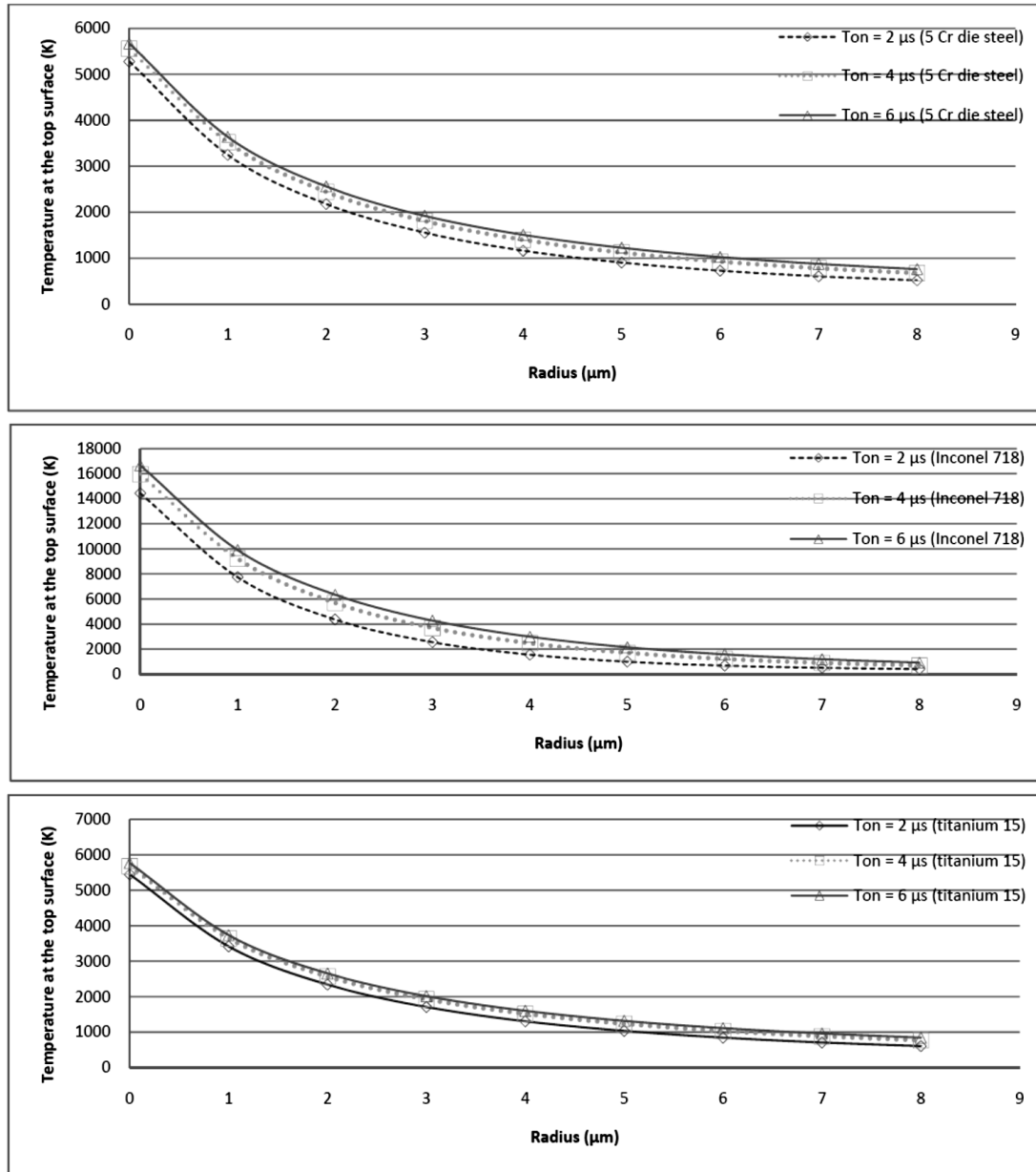


Figure 40 The effect of pulse duration on the temperature distribution along the radial direction from the centerline for micro EDM at  $P = 0.08$ ,  $I = 1.5$  A,  $V = 20$  V.



**Figure 41** The effect of pulse duration on the temperature distribution along the depth of workpiece at the centerline for micro EDM at  $P = 0.08$ ,  $I = 1.5$  A,  $V = 20$  V.

### 5.7.3 Effect of heat input to the workpiece

The effect of variation of heat input to the workpiece along the radius and depth are shown in Fig. 42 and 43. From both figures, it can be observed that higher surface temperature is attained at high value of energy portion.

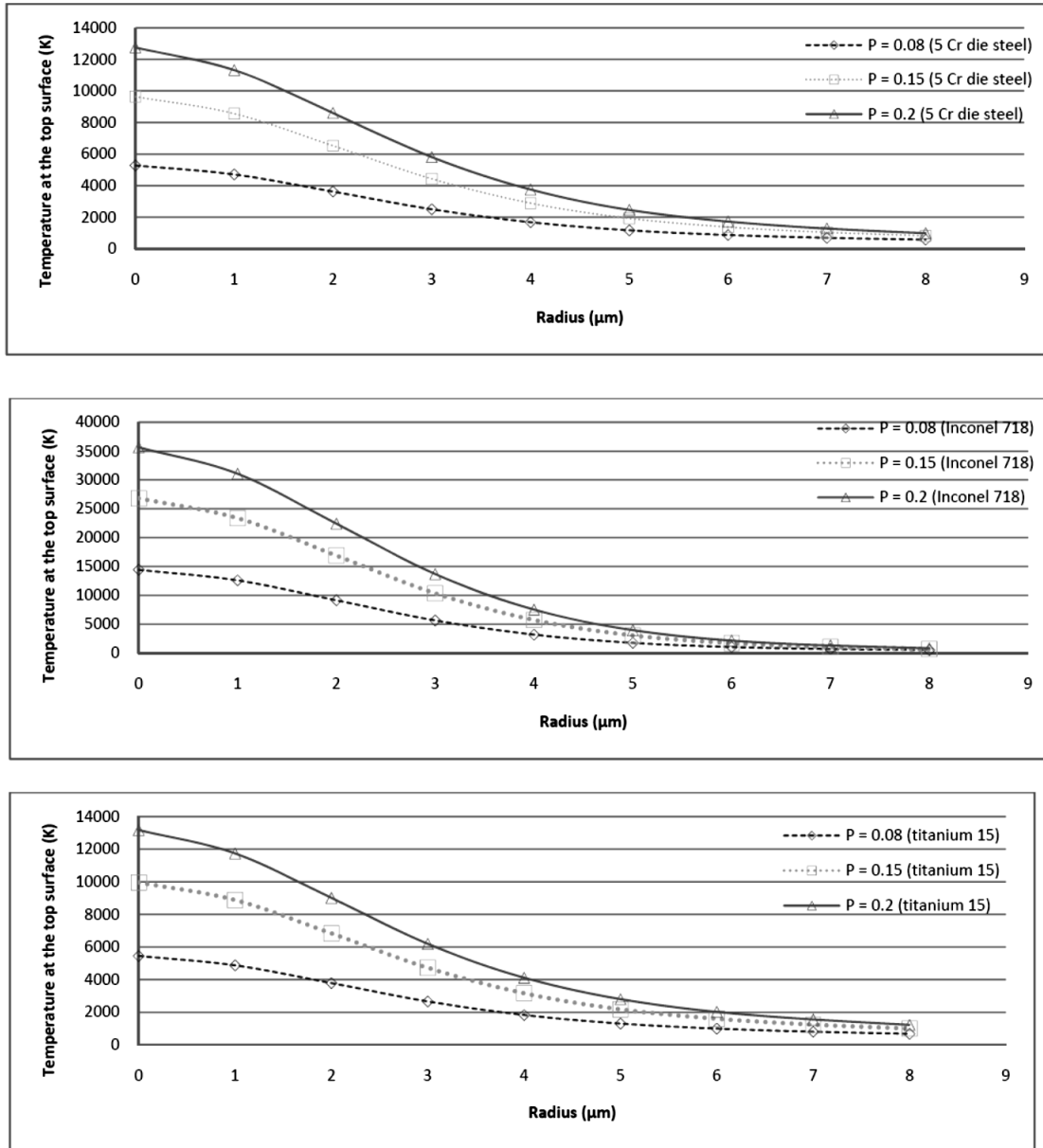


**Figure 42** The effect of heat input to the workpiece on the temperature distribution along the radial direction from the centerline for micro EDM at  $I = 1.5 \text{ A}$ ,  $T_{on} = 2 \text{ μs}$ ,  $V = 20\text{V}$

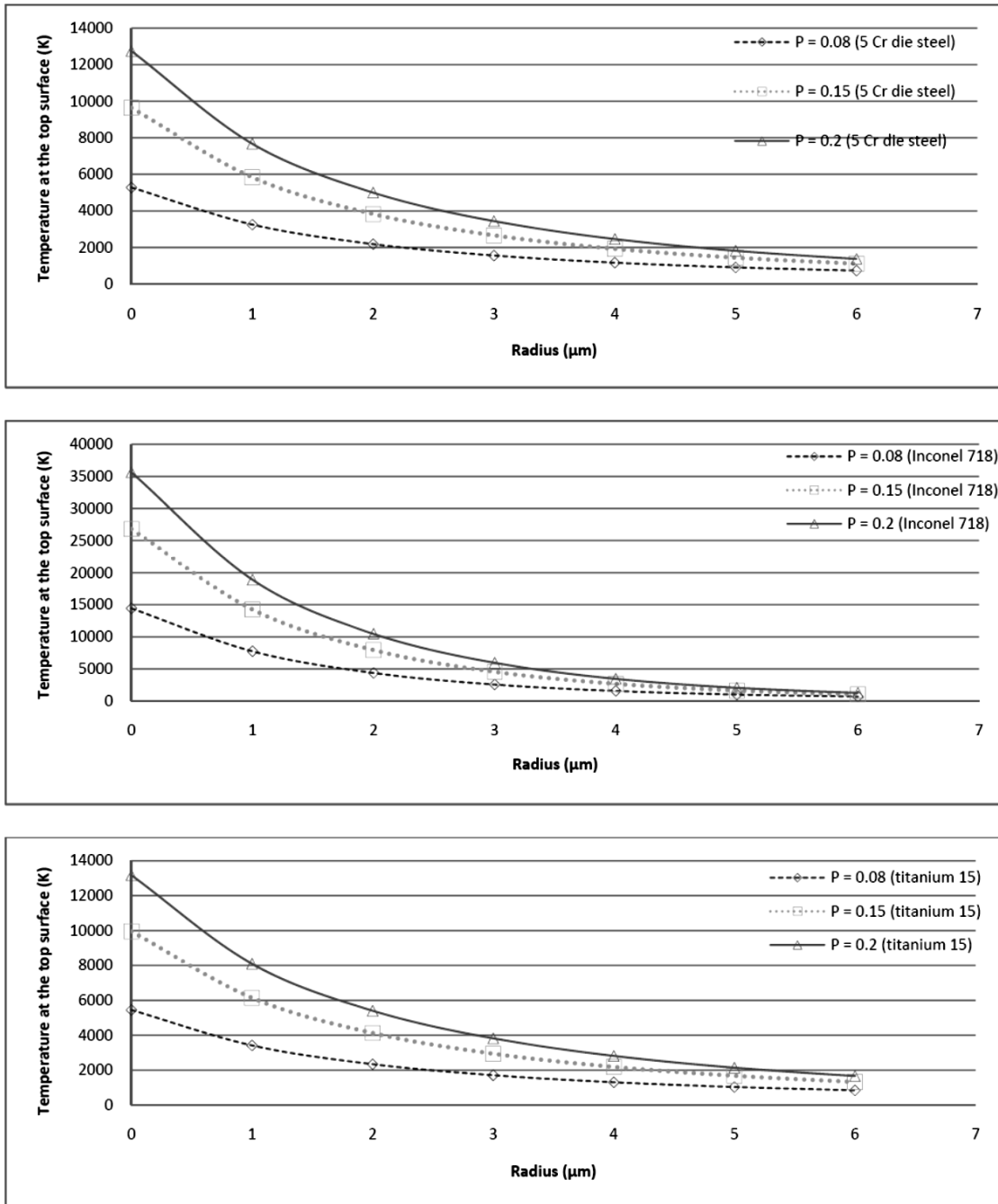


**Figure 43** The effect of heat input to the workpiece on the temperature distribution along the depth of workpiece at the centerline for micro EDM at  $I = 1.5$  A,  $T_{on} = 2$  μs,  $V = 20$  V.

# Chapter 6

**CONCLUSIONS**



## 6 Conclusions

### ➤ For Micro EDM Experiment

- From the S/N ratio plot the optimum parameter settings are  $V_{III}T_{on}^2$ , ie.  $V = 2V$ ,  $I = 3A$  and  $T_{on} = 4\mu s$ .
- It can also be observed that  $T_{on}$  is the most prominent factor affecting the responses.

### ➤ For ANSYS Model For EDM Extended To Micro EDM

- Firstly EDM simulation for 5 Cr die steel has been performed then it is extended for the micro EDM process, for single pulse, on different workpiece materials. The effects of different process parameters have also been studied. For micro EDM process MRR also have been calculated for Inconel 718 and Titanium 15.
- From the MRR analysis it has been found that Inconel 718 gives a much higher MRR compare to Titanium 15.
- It can also be observed from the graphs that current is most prominent factor, having significant effect on heat flux.
- Optimum parameter setting is Voltage = 15 V, Current = 5A and heat input to the workpiece = 0.15.

### ➤ For FEA Modelling of Multi-discharge Micro EDM

- For multi-discharge error in MRR found to be about 25.98%.

## REFERENCES

## References

- [1]. T. Masuzawa and H. K. Tonshoff, —"Three-dimensional micromachining by machine tools", *Annals of the CIRP* (1997) 46 (2), 621-628.
- [2]. T. Masuzawa, —State of the art micro-machining, *Annals of the CIRP* (2000) 49 (2) 621- 628.
- [3]. T. Masuzawa, —State of the art micro-machining, *Annals of the CIRP* (2000) 49 (2) 473-488.
- [4]. Muhammad Pervej Jahan, Yoke San Wong, Mustafizur Rahman, —A comparative experimental investigation of deep-hole micro-EDM drilling capability for cemented carbide (WC-Co) against austenitic stainless steel (SUS 304), *International Journal of Advance Manufacturing Technology* (2010) 46:1145–1160
- [5]. D. Reynaerts, W. Meeusen, X. Song, H. V. Bruseel, S. Reyntjens, D. D. Bruyker, and R. Puers, "Integrating electro-discharge machining and photolithography: Work in progress," *J. Micromech. Microeng.*, vol. 10, no. 2, pp. 189–195, June 2000.
- [6]. [37] Y. Honma, K. Takahashi, and M. Muro, "Micro-machining of magnetic metal film using electro-discharge technique," *Adv. Inform. Stor.Syst.*, vol. 10, pp. 383–399, 1999.
- [7]. [38] C. A. Grimes, M. K. Jain, R. S. Singh, Q. Cai, A. Mason, K. Takahata, and Y. Gianchandani, "Magnetoelastic microsensors for environmental monitoring," in *Tech. Dig. IEEE Int. Conf. Micro Electro Mechanical Systems (MEMS'01)*, Interlaken, Switzerland, Jan. 2001, pp. 278–281.
- [8]. K. Fischer, B. Chaudhuri, S. McNamara, H. Guckel, Y. Gianchandani, and D. Novotny, "A latching, bistable optical fiber switch combining LIGA technology with micromachined permanent magnets," in *Tech. Dig., IEEE Intl. Conf. on Solid-State Sensors and Actuators (Transducers' 01)*, Munich, Germany, June 2001, pp. 1340–1343.
- [9]. Katz Z., Tibbles C.J. "Analysis of Micro-scale EDM process", *International Journal of Advanced Manufacturing Technologies*, 25 (2005) - 923-928.
- [10]. Masuzawa T., "Micro EDM". *Proceedings of the ISEM XIII* (2001).3-19. Fundación Tekniker. ISBN 932064-0-7.

- [11]. Masuzawa T., “State of the Art Micromachining”. *Annals of CIRP* Vol 49/02/2000. 473-488
- [12]. Albert M. “Fine Wire is just Fine”, *Modern Machine Shop On-line* – Gardner Publications Inc. – <http://www.msonline.com/articles/099904.html>
- [13]. G. Kibria & B. R. Sarkar & B. B. Pradhan & B. Bhattacharyya. —Comparative study of different dielectrics for micro-EDM performance during microhole machining of Ti-6Al-4V alloy”, *Int J Adv Manuf Technol* (2010) 48:557–570.
- [14]. O. Koch, W. Ehrfeld, F. Michel and H.P. Gruber, —Recent progress in micro-electro discharge machining technology-part-1, *Proceedings of the 13th International Symposium for Electro machining ISEM XIII*, Bilbao, Spain (2001).
- [15]. Mark T. Richardson, Yogesh B. Gianchandani and Dawn S. Skala, —A parametric study of dimensional tolerance and hydrodynamic debris removal in micro-electro-discharge machining”, *MEMS 2006*, Istanbul, Turkey
- [16]. Mark T. Richardson, and Yogesh B. Gianchandani, —Wireless Monitoring of Workpiece Material Transitions and Debris Accumulation in Micro-Electro-Discharge Machining”, *Journal of microelectromechanical systems*, vol. 19, no. 1, february 2010
- [17]. Schumacher B.M., —After 60 Years of EDM the Discharge Process Remains Still Disputed”, *Journal of Material Processing Technology* (2004) 149; 376-381.
- [18]. E. Bud Guitrau, —The EDM Handbook 1997, Section 4, 1997 (Chapter 19).
- [19]. Han-Ming Chow, Lieh-Dai Yang, Ching-Tien Lin and Yuan-Feng Chen, —The use of SiC powder in water as dielectric for micro-slit EDM machining”, *Journal of materials processing technology* 195(2008)160–170
- [20]. Gunawan Setia Prihandana, Muslim Mahardika, M. Hamdi, Y.S. Wong and Kimiyuki Mitsui, —Effect of micro-powder suspension and ultrasonic vibration of dielectric fluid in micro- EDM processes—Taguchi approach”, *International Journal of Machine Tools & Manufacture* 49 (2009) 1035–1041
- [21]. Muhammad Pervej Jahan, Mustafizur Rahman and Yoke San Wong, —Study on the nanopowder- mixed sinking and milling micro-EDM of WC-Co, *International Journal of Advance Manufacturing Technology*, DOI 10.1007/s00170-010-2826-9 (2010)

- [22]. Jean Bosco Byiringiro, Bernard W. Ikua and George N. Nyakoe, Fuzzy Logic Based Controller for Micro-Electro Discharge Machining Servo Systems, IEEE AFRICON 2009
- [23]. B.H. Yan, A.C. Wang, C.Y. Huang and F.Y. Huang, —Study of precision micro-holes in borosilicate glass using micro EDM combined with micro ultrasonic vibration machining”, International Journal of Machine Tools & Manufacture 42 (2002) 1105–1112
- [24]. Kenichi Takahata and Yogesh B. Gianchandani, —Batch Mode Micro-Electro-Discharge Machining”, Journal of micro electromechanical systems, vol. 11, no. 2, April 2002
- [25]. Feng-Tsai Weng, R.F. Shyu and Chen-Siang Hsu, —Fabrication of micro-electrodes by multi-EDM grinding process”, Journal of Materials Processing Technology 140 (2003) 332–334
- [26]. Hideki Takezawa, Hiroaki Hamamatsu, Naotake Mohri and Nagao Saito, —Development of micro-EDM-centre with rapidly sharpened electrode, Journal of Materials Processing Technology 149 (2004) 112–116
- [27]. A Cheng Wang, BiingHwa Yan, You Xi Tang and Fuang Yuan Huang, —The feasibility study on a fabricated micro slit die using micro EDM”, International Journal of Advance Manufacturing Technology (2005) 25: 10–16
- [28]. Sang Min Yi, Min Soo Park, Young Soo Lee and Chong Nam Chu, —Fabrication of a stainless steel shadow mask using batch mode micro-EDM”, Microsyst Technol (2008) 14:411–417
- [29]. M.P. Jahan, Y.S. Wong and M. Rahman, —A study on the fine-finish die-sinking micro- EDM of tungsten carbide using different electrode materials”, journal of materials processing technology 209 (2009) 3956–3967
- [30]. Dinesh Rakwal, Sumet Heamawatana chai, Prashant Tathireddy, Florian Solzbacher and Eberhard Bamberg, —Fabrication of compliant high aspect ratio silicon microelectrode arrays using micro-wire electrical discharge machining”, Microsyst Technol (2009) 15:789–797

- [31]. Yang-Yang Hu, D. Zhu, N. S. Qu, Y. B. Zeng and P. M. Ming, Fabrication of high-aspect ratio electrode array by combining UV-LIGA with micro electro-discharge machining, *Microsyst Technol* (2009) 15:519–525
- [32]. Eberhard Bamberg and Sumet Heamawatanachai, —Orbital electrode actuation to improve efficiency of drilling micro-holes by micro-EDM, *Journal of Materials Processing Technology* 209 (2009) 1826–1834
- [33]. Ornwas Traisigkhachol, Hermann Schmid Marc Wurz and Hans H. Gatzert, —Applying SU-8 to the fabrication of micro electro discharge machining electrodes, *Microsyst Technol* (2010) 16:1445–1450
- [34]. G. Girardin, Y. Layouni, P. Morin and M. Cabrera, —Micro EDM With The In Situ Electrochemical Fabrication And Regeneration Of The Tungsten Microelectrode Tool”, *International Journal of Material Forming* (2010) Vol. 3 Suppl 1:1083 – 1086
- [35]. O. Blatnik, J. Valentincic and M. Junkar, —Comparison of optimal machining parameters of sinking EDM and micro EDM processes, *Multi-material Micro Manufacture*, 2005 elsevier.
- [36]. Pham DT, Ivanov A, Bigot S, Popov K, Dimov S, —An investigation of tube and rod electrode wear in micro EDM drilling, *International Journal of Advance Manufacturing Technology* 33(1–2) (2007):103–109
- [37]. Changshui Gao and Zhengxun Liu, —A study of ultrasonically aided micro-electrical discharge machining by the application of workpiece vibration, *Journal of Materials Processing Technology* 139 (2003) 226–228
- [38]. Philip Allen, Xiaolin Chen, —Process simulation of micro electro-discharge machining on molybdenum”, *Journal of Materials Processing Technology* 186 (2007) 346–355
- [39]. Guanrong Hang, Guohui Cao, Zaicheng Wang, Jing Tang, Zhenlong Wang and Wansheng Zhao, —Micro-EDM Milling of Micro Platinum Hemisphere, *Proceedings of the 1st IEEE International Conference on Nano/Micro Engineered and Molecular Systems* January 18 - 21, 2006, Zhuhai, China
- [40]. B. B. Pradhan, M. Masanta, B. R. Sarkar and B. Bhattacharyya, —Investigation of electro discharge micro-machining of titanium super alloy, *International Journal of Advance Manufacturing Technology* (2009) 41:1094–1106

- [41]. LI Mao-sheng, CHI Guan-xin, WANG Zhen-long, WANG Yu-kui and DAI Li, —Micro electrical discharge machining of small hole in TC4 alloy, trans. Nonferrous Met. Soc. China 19 (2009) 434-439
- [42]. Kunieda M, Lauwers B, Rajurkar K, Schumacher BM (2005) Advancing EDM through fundamental insight into the process. CIRP Ann 54(2):599–622. doi:10.1016/S0007-8506(07)60020-1
- [43]. Fuzhu Han, Shinya Wachi and Masanori Kunieda, —Improvement of machining characteristics of micro-EDM using transistor type isopulse generator and servo feed control”, Precision Engineering 28 (2004) 378–385
- [44]. Masuzawa T, Fujino M (1980) Micro pulse for EDM. Proc Japan Society for Precision Engineering Autumn Conference, pp 140–142
- [45]. Fuzhu Han, Li Chen, Dingwen Yu and Xiaoguang Zhou, —Basic study on pulse generator for micro-EDM”, International Journal of Advance Manufacturing Technology (2007) 33: 474–479
- [46]. Seong Min Son, Han Seok Lim, A.S. Kumar and M. Rahman, —Influences of pulsed power condition on the machining properties in micro EDM”, Journal of Materials Processing Technology 190 (2007) 73–76
- [47]. Aditya Shah, Vishal Prajapati, Pavan Patel and Akash Pandey, —Development of Pulsed Power Dc Supply for Micro EDM”, UGC National Conference on Advances in Computer Integrated Manufacturing (NCACIM) February 16-17, 2007.
- [48]. Horowitz P. and Hill W, —The Art of Electronics”, Cambridge University Press, 1989, 0-521-49846-5.
- [49]. Mu-Tian Yan and Tsung-Liang Chiang, —Design and experimental study of a power supply for micro-wire EDM”, International Journal of Advance Manufacturing Technology (2009) 40:1111–1117
- [50]. H. Xia, M. Kunieda and N. Nishiwaki, —Removal Amount Difference between Anode and Cathode in EDM Process”, IJEM, 1 (1996), pp. 45-52
- [51]. Fuzhu Han, Yuji Yamada, Taichi Kawakami, and Masanori Kunieda, —Experimental attempts of sub-micrometer order size machining using micro-EDM”, Precision Engineering 30 (2006) 123–131

- [52]. Higuchi T, Furutani K, Yamagata Y and Takeda K., —Development of pocket size electro discharge machine”. *Annals of the CIRP* 1991; 40(1):203–6.
- [53]. Morita H., Furutani K. and Mohri N., —Electrical discharge device with direct drive method for thin wire electrode”, *Proceedings of IEEE International Conference on Robotics and Automation*, 1995:73–78.
- [54]. Yong Li, Min Guo, Zhaoying Zhou and Min Hu, —Micro electro discharge machine with an inchworm type of micro feed mechanism”, *Journal of the International Societies for Precision Engineering and Nanotechnology* 26 (2002) 7–14
- [55]. Hao Tong, Yong Li, Yang Wang and Dingwen Yu, —Servo scanning 3D micro-EDM based on macro/micro-dual-feed spindle”, *International Journal of Machine Tools & Manufacture* 48 (2008) 858–869
- [56]. Muralidhara, Nilesh J. Vasa and SingaperumalMakarama, —Investigations on a directly coupled piezoactuated tool feed system for micro-electro-discharge machine”, *International Journal of Machine Tools & Manufacture* 49 (2009) 1197–1203
- [57]. JianwenGuo, Xiaofei Chen and Masanori Kunieda, —Molecular Dynamics Simulation of the Material Removal Mechanism in Micro-EDM”, *Precision Engineering Article in Press*
- [58]. Murali M. Sundaram, Ganesh B. Pavalarajan, and Kamlakar P. Rajurkar, —A Study on Process Parameters of Ultrasonic Assisted Micro EDM Based on Taguchi Method”, *JMEPEG* (2008) 17:210–215
- [59]. A. Guha, S. Smyers, K.P. Rajurkar, P.S. Garinella and R. Konda, —Optimal parameters in electrical discharge machining of copper - beryllium alloys”, *Proceedings of the International Symposium for Electro machining, ISEM XI, April 17 - 21, 1995, EPFL, Lausanne, Switzerland*, pp. 217 - 224.
- [60]. B.H. Yan, H.C. Tsai and Y.C. Lin, —Study on EDM characteristics of cemented carbides”, in: *Proceedings of the 14th National Conference on Mechanical Engineering*, The Chinese Society of Mechanical Engineers, 1997, pp. 157 - 164.
- [61]. Kung KY, Horng JT and Chiang KT, —Material removal rate and electrode wear ratio study on the powder mixed electrical discharge machining of cobalt-bonded tungsten carbide”, *International Journal of Advance Manufacturing Technology*, 40:95–104 (2009)



- [62]. L. Chen, E. Siores and W. Wong, —Kerf characteristics in abrasive water jet cutting of ceramic materials”, *Int. J. Mach. Tools Manufact.* 36(11) (1996) 1201-1206.
- [63]. W.S. Lau and W.B. Lee, —A comparison between EDM wire cut and laser cutting of carbon fibre composite materials”, *Mater. Manufacturing Process* 6(2) (1991) 331-342.
- [64]. G. Spur and S. Hall, —Ultrasonic assisted grinding of ceramics”, in: *Conference on Precision Engineering, 2nd ICMT, Singapore, 1995*, pp. 52-55.
- [65]. H.K. Tonshoff and C. Emmelmann, —Laser cutting of advanced ceramics”, *Ann. CIRP* 38(1) (1989) 219-222.
- [66]. Tzeng Yih-fong and Chen Fu-chen, —Investigation into some surface characteristics of electrical discharge machined SKD-11 using powder-suspension dielectric oil”, *Journal of Materials Processing Technology* 170 (2005) 385–391
- [67]. Hung Sung Liu, BingHwa Yan, Chien Liang Chen and Fuang Yuan Huang, *Application of micro-EDM combined with high-frequency dither grinding to micro-hole machining”, International Journal of Machine Tools & Manufacture* 46 (2006) 80–87
- [68]. Yu ZY, Masuzawa T, Fujino M, —Micro-EDM for three dimensional cavities—development of uniform wear method”, *Annals CIRP* 47(1): 169–172 (1998)
- [69]. Bleys P, Kruth JP, Lauwers B, Zryd A, Delpretti R, Tricarico C, —Real-time tool wear compensation in milling EDM”, *Annals CIRP* 51(1):157–160 (2002)
- [70]. Dauw D, —On the derivation and application of a real time tool wear sensor in EDM”. *Annals CIRP* 35(1):111–116, (1986)
- [71]. Mu-Tian Yan, Kuo-Yi Huang, Chin-Yen Lo, —A study on electrode wear sensing and compensation in Micro-EDM using machine vision system”, *International Journal of Advance Manufacturing Technology* (2009) 42:1065–1073
- [72]. Yu ZY, Masuzawa T, Fujiino M, —3D micro-EDM with simple shape electrode”, Part 1. *Int J Electr Mach* 3:7–12 (1998)
- [73]. Yu ZY, Masuzawa T, Fujiino M, —3D micro-EDM with simple shape electrode”, Part 2. *Int J Electr Mach* 3:71–79 (1998)
- [74]. Rajurkar KP, Yu ZY, —3D micro-EDM using CAD/CAM”, *CIRP Ann* 49(1):127–130 (2000)

- [75]. Yu ZY, Kozak J, Rajurkar KP, —Modelling and simulation of micro EDM process”, CIRP Ann 52(1):143–146 (2003)
- [76]. Kozak J, Ivanov A, Al-naemi F, Gulbinowicz Z, —EDM electrode wear and its effect on processes accuracy and process modelling”, In: Proceedings of the 15th International Symposium on Electro machining (ISEM-15), pp 81–86 (2007)
- [77]. S.H. Yeo and P.C. Tan, —A New Tool Wear Compensation Method based on Real Time Estimation of Material Removal Volume in Micro EDM”, Journal of Materials Processing Technology Article in Press
- [78]. EckartUhlmann and Markus Roehner, —Investigations on reduction of tool electrode wear in micro-EDM using novel electrode materials”, CIRP Journal of Manufacturing Science and Technology 1 (2008) 92–96
- [79]. Wang Yuangang, Zhao Fuling, Wang Jin, —Wear-resist Electrodes for Micro-EDM”, Chinese Journal of Aeronautics 22(2009) 339-342
- [80]. EckartUhlmann, Stefan Rosiwal, Katharina Bayerlein and Markus Rohner, —Influence of grain size on the wear behaviour of CVD diamond coatings in micro-EDM”, International Journal of Advance Manufacturing Technology (2010) 47:919–922.
- [81]. K. Takahata, N. Shibaike and H. Guckel, —High-aspect-ratio WC-Co microstructure produced by the combination of LIGA and Micro-EDM”, Microsystem Technologies 6 (2000) 175-178
- [82]. T. Masuzawa, J. Tsukamoto and M. Fujino, —Drilling of deep microholes by EDM”, Annals CIRP, 38 (1), pp. 195–198, 1989.
- [83]. A. Schoth, R. Forster and W. Menz, —Micro wire EDM for high aspect ratio 3D micro structuring of ceramics and metals”, Microsystem Technologies 11 (2005) 250–253 Springer- Verlag 2005
- [84]. D. M. Cao, J. Jiang, W. J. Meng, J. C. Jiang and W. Wang, —Fabrication of high-aspect ratio micro scale Ta mold inserts with micro electrical discharge machining”, MicrosystTechnol (2007) 13: 503–510
- [85]. Yeo S H, Tan L K, —Effects of ultrasonic vibrations in micro electro-discharge machining of micro holes. Journal of Micromech. Microeng. 1999; 9: 345-352

- [86]. Masuzawa, T. and Heuvelman, C. J., Self flushing method with spark-erosion machining. *CIRP Annals - Manufacturing Technology*.1983; 32: 109-111.
- [87]. Masuzawa, T., Cui X. X. and Fujino M., —A New Flushing Method for EDM Die sinking - Effect of 2d Small Vibration of the Electrode. *Bulletin of the Japan Society of Precision Engineering*.1990; 24: 223-224.
- [88]. Yeo, S. H. and Goh, K. M. The effect of ultrasound in micro electro discharge machining on surface roughness. *Proceedings of the Institution of Mechanical Engineers Part B-Journal of Engineering Manufacture*.2001; 215: 271-276.
- [89]. Huang, H., Zhang, H., Zhou, L. and Zheng, H. Y. —Ultrasonic vibration assisted electrodischarge machining of micro holes in Nitinol. *Journal of Micromechanics and Microengineering*.2003; 13: 693-700.
- [90]. Mu-Tian Yan, Chen-Wei Huang, Chi-Cheng Fang and Chia-Xuan Chang, —Development of a prototype Micro-Wire-EDM machine, *Journal of Materials Processing Technology* 149 (2004) 99–105
- [91]. Changshui Gao and Zhengxun Liu, —A study of ultrasonically aided micro-electrical discharge machining by the application of workpiece vibration, *Journal of Materials Processing Technology* 139 (2003) 226–228
- [92]. K. Takahata, N. Shibaike and H. Guckel, —High-aspect-ratio WC-Co microstructure produced by the combination of LIGA and Micro-EDM, *Microsystem Technologies* 6 (2000) 175-178
- [93]. C. L. Kuo, J. D. Huang and H. Y. Liang, —Precise Micro-Assembly Through an Integration of Micro-EDM and Nd-YAG”, *International Journal Advance Manufacturing Technology* (2002) 20: 454–458
- [94]. Ivano Beltrami, Cedric Joseph, Reymond Clavel, Jean-Philippe Bacher and Stefano Bottinelli, —Micro and nanoelectric discharge machining, *Journal of Materials Processing Technology* 149 (2004) 263–265
- [95]. Guo Rui, Zhao Wansheng and LI Gang, —Development of a CNC micro-EDM machine”, *Advanced Manufacturing Technology, International Technology and Innovation Conference* 2006

- [96]. Gwo-LianqChern, Ying-JengEngin Wu and Shun-Feng Liu, —Development of a micro punching machine and study on the influence of vibration machining in micro-EDM”, *Journal of Materials Processing Technology* 180 (2006) 102–109
- [97]. Yang-Yang Hu, D. Zhu, N. S. Qu, Y. B. Zeng and P. M. Ming, Fabrication of high-aspectratio electrode array by combining UV-LIGA with micro electro-discharge machining, *MicrosystTechnol* (2009) 15:519–525
- [98]. Z.Y. Yu, Y. Zhang, J. Li, J. Luan, F. Zhao and D. Guo, —High aspect ratio micro-hole drilling aided with ultrasonic vibration and planetary movement of electrode by micro-EDM”, *CIRP Annals - Manufacturing Technology* 58 (2009) 213–216
- [99]. PengZilong, Wang Zhenlong, Dong Yinghuai and Chen Hui, —Development of a reversible machining method for fabrication of microstructures by using micro-EDM”, *Journal of Materials Processing Technology* 210 (2010) 129–136
- [100]. Chang-Sheng Lin, Yunn-Shiuan Liao, Yi-Ting Cheng and Yunn-Cheng Lai, Fabrication of micro ball joint by using micro-EDM and electroforming, *Microelectronic Engineering* 87 (2010) 1475–1478
- [101]. P. Shankar, V.K. Jain, T. Sundarajan, Analysis of spark profiles during EDM process, *Machining Science and Technology* 1 (2) (1997) 195–217.
- [102]. M. Kunieda, K. Yanatori, Study on debris movement in EDM gap, *International Journal of Electrical Machining* 2 (1997) 43–49.
- [103]. Y.F. Luo, The dependence of interspace discharge transitivity upon the gap debris in precision electro-discharge machining, *Journal of Materials Processing Technology* 68 (1997) 127–131.
- [104]. K Furutani, A. Saneto, H. Takezawa, N. Mohri, H. Miyake, Accertation of titanium carbide by electrical discharge machining with powdersuspended in working fluid, *Precision Engineering* 25 (2001) 138–144.
- [105]. Yih-fongTzeng, Chen Fu-chen, A simple approach for robust design of high-speed electrical-discharge machining technology, *International Journal of Machine Tool & Manufacture* 43 (2003) 217–227.
- [106]. D.D. DiBitonto, P.T. Eubank, M.R. Patel, M.A. Barrufet, Theoretical models of the electrical discharge machining process. I. A simple cathode erosion model, *Journal of Applied Physics* 66 (9) (1989) 4095–4103.

- [107]. M.R. Patel, A. Barrufet, P.T. Eubank, D.D. DiBitonto, Theoretical models of the electrical discharge machining process—II: The anode erosion model, *Journal of Applied Physics* 66 (9) (1989) 4104–4111.
- [108]. P.E. Eubank, M.R. Patel, M.A. Barrufet, B. Bozkurt, Theoretical models of the electrical discharge machining process. III. The variable mass, cylindrical plasma model, *Journal of Applied Physics* 73 (11) (1993) 7900–7909.
- [109]. R. Bhattacharya, V.K. Jain, P.S. Ghoshdastidar, Numerical simulation of thermal erosion in EDM process, *IE (I) Journal-PR* 77 (1996) 13–19.
- [110]. V. Yadav, V. Jain, P. Dixit, Thermal stresses due to electrical discharge machining, *Int. J. Mach. Tools Manuf.* 42 (2002) 877–888.
- [111]. Shuvra Das, Mathias Klotz and F. Klocke, EDM simulation: finite element-based calculation of deformation, microstructure and residual stresses, *Journal of Materials Processing Technology* 142 (2003) 434–451